The FASEB Journal
The Journal of the Federation of American Societies for Experimental Biology
All Articles | Submit | Subscribe | What's New | RSS

FASEB J. 2018 Jul; 32(7): 3623–3640. PMCID: PMC5998970
Published online 2018 Feb 8. doi: 10.1096/fj.201701176R: 10.1096/fj.201701176R PMID: 29452565

Serum vitamin C levels modulate the lifespan and endoplasmic reticulum stress response pathways in mice synthesizing a nonfunctional mutant WRN protein

Lucie Aumailley,[*] Marie Julie Dubois,[†] Tracy A. Brennan,[‡] Chantal Garand,[*] Eric R. Paquet,[§] Robert J. Pignolo,[¶] André Marette,[†] and Michel Lebel[*,1]

[*]Centre de Recherche du Centre Hospitalier de l'Université (CHU) de Québec, Faculté de Médecine, Université Laval, Quebec City, Quebec, Canada;
[†]Institut Universitaire de Cardiologie et de Pneumologie de Québec, Faculté de Médecine, Université Laval, Quebec City, Quebec, Canada;
[‡]Department of Medicine, Perelman School of Medicine, University of Pennsylvania, Philadelphia, Pennsylvania, USA;
[§]Centre de Recherche sur le Cancer de l'Université Laval, Hôpital Hôtel-Dieu de Québec, Quebec City, Quebec, Canada
[¶]Department of Medicine, Mayo Clinic College of Medicine, Rochester, Minnesota, USA
[1]Correspondence: Centre de Recherche du CHU de Quebec, Centre Hospitalier de l'Université Laval, 2705 Laurier Blvd., Local T-2-04, Quebec City, Quebec G1V 4G2, Canada., E-mail: michel.lebel@crchudequebec.ulaval.ca

Received 2017 Oct 20; Accepted 2018 Jan 22.

Abstract

Werner syndrome (WS) is a premature aging disorder caused by mutations in a RecQ-family DNA helicase (WRN). Mice lacking part of the helicase domain of the WRN ortholog exhibit several phenotypic features of WS. In this study, we generated a Wrn mutant line that, like humans, relies entirely on dietary sources of vitamin C (ascorbate) to survive, by crossing them to mice that lack the gulonolactone oxidase enzyme required for ascorbate synthesis. In the presence of 0.01% ascorbate (w/v) in drinking water, double-mutant mice exhibited a severe reduction in lifespan, small size, sterility, osteopenia, and metabolic profiles different from wild-type (WT) mice. Although increasing the dose of ascorbate to 0.4% improved dramatically the phenotypes of double-mutant mice, the metabolic and cytokine profiles were different from age-matched WT mice. Finally, double-mutant mice treated with 0.01% ascorbate revealed a permanent activation of all the 3 branches of the ER stress response pathways due to a severe chronic oxidative stress in the ER compartment. In addition, markers associated with the ubiquitin-proteasome–dependent ER-associated degradation pathway were increased. Augmenting the dose of ascorbate reversed the activation of this pathway to WT levels rendering this pathway a potential therapeutic target in WS.—Aumailley, L., Dubois, M. J., Brennan, T.

A., Garand, C., Paquet, E. R., Pignolo, R. J., Marette, A., Lebel, M. Serum vitamin C levels modulate the lifespan and endoplasmic reticulum stress response pathways in mice synthesizing a non-functional mutant WRN protein.

Keywords: Werner syndrome, ascorbate, metabolomic, gulonolactone oxidase, aging

Werner syndrome (WS) is a human autosomal recessive disorder characterized by genomic instability and the premature onset of several age-related diseases (1–4). The defective enzyme responsible for WS is a DNA exonuclease/helicase involved in DNA repair, replication, transcription, and telomere maintenance (5–9). Several years ago, we generated a mouse model with a deletion in the helicase domain of the murine WS RecQ-like helicase gene (*Wrn*) ortholog (10) (referred to as $Wrn^{\Delta hel/\Delta hel}$, hereafter). This deletion abolishes both the helicase and exonuclease activities of the mouse Wrn protein (11). $Wrn^{\Delta hel/\Delta hel}$ mice develop abnormally high visceral fat content, hepatic steatosis (12), and aortic stenosis followed by cardiac fibrosis (13). In addition, $Wrn^{\Delta hel/\Delta hel}$ mice show an increase in genomic instability with age, an increase in the incidence of several cancer types, and a reduced mean lifespan of ~17% compared with wild-type (WT) mice (14, 15). Similar to patients with WS (16), the antioxidant status (levels of vitamin C or ascorbate and glutathione) in 9-mo-old $Wrn^{\Delta hel/\Delta hel}$ mice is abnormally high in blood compared with age-matched WT mice (15). This difference suggests that $Wrn^{\Delta hel/\Delta hel}$ mice are trying to cope with an unbalanced cellular redox status or that the Wrn protein affects genes involved in the oxidative stress response (17). Accordingly, we found that untreated $Wrn^{\Delta hel/\Delta hel}$ mouse embryonic fibroblast redox status is similar to WT mouse embryonic fibroblasts that have been treated with hydrogen peroxide (18). We tested the impact of 3 known antioxidants (catechin, resveratrol, and ascorbate) on the health of $Wrn^{\Delta hel/\Delta hel}$ mice (12, 15, 19). Surprisingly, the most efficient antioxidant in reversing the observed phenotypes in $Wrn^{\Delta hel/\Delta hel}$ mice was ascorbate, despite the fact that mice, unlike humans, synthesize their own ascorbate (15). In this study, we generated $Wrn^{\Delta hel/\Delta hel}$ mice that, like humans, rely entirely on diet to obtain ascorbate, to better assess the impact of ascorbate on this mouse model. The murine enzyme (absent in humans) required for *de novo* ascorbate synthesis is the gulonolactone oxidase encoded by the *Gulo* gene. Without ascorbate supplementation in their diet, *Gulo* null ($Gulo^{-/-}$) mice become rapidly sick, similar to humans (20). We examined the effect of 0.01 and 0.4% (w/v) ascorbate supplementation in drinking water on $Wrn^{\Delta hel/\Delta hel}/Gulo^{-/-}$ mice. A 0.4% ascorbate supplementation has been shown to significantly extend the lifespan of $Wrn^{\Delta hel/\Delta hel}$ mice (21).

MATERIALS AND METHODS

Mice

$Gulo^{-/-}$ mice were obtained from the Mutant Mouse Regional Resource Centers (University of California–Davis, Davis, CA, USA) and were housed at the Centre de Recherche en Cancérologie de l'Université Laval animal facility. Mice lacking part of the helicase domain of the *Wrn* gene were generated by homologous recombination (10). All mice were backcrossed onto C57BL/6 background for 12 generations. Mice of all required genotypes were obtained by mating homozygous $Wrn^{\Delta hel/\Delta hel}$ individuals with $Gulo^{-/-}$ mice and intercrossing the F1 and F2 generations. Care of mice was in accordance with the guidelines of Laval University's Animal Protection Committee (Permit 2014029). Mice were housed in cages (containing a top filter)

on static racks in a conventional animal facility at 22 ± 2°C with 40–50% humidity and a 12-h light–dark cycle (light cycle: 06:00–18:00 h). All mice were fed *ad libitum* with the standard 2018 Teklad Global 18% Protein Rodent Diet (Envigo, Madison, WI, USA). Mice were checked every day, and those that became immobile or moribund were euthanized for histologic examination of their organs (14). Euthanasia was performed with 3% isoflurane (general anesthesia) followed by cervical dislocation. One cohort of $Gulo^{-/-}$ mice and 1 cohort of $Wrn^{\Delta hel/\Delta hel}/Gulo^{-/-}$ mice were maintained on a standard diet and supplemented with 0.01% of L-ascorbate (w/v) in drinking water from weaning until the ages indicated in the analyses. A second cohort of $Wrn^{\Delta hel/\Delta hel}/Gulo^{-/-}$ mice was given 0.4% L-ascorbate (w/v) in drinking water for the various times indicated. WT control C57BL/6 mice were maintained in the same room from weaning until the age of 4 or 20 mo with normal drinking water (no ascorbate supplement). Finally, $Wrn^{\Delta hel/\Delta hel}$ mutant mice were maintained under standard diet with no ascorbate supplementation.

Histologic examination

Tissues were fixed in 4% paraformaldehyde and embedded in paraffin. Thin sections were mounted on glass slides and stained with hematoxylin and eosin (H&E). TUNEL assays for detection of apoptotic cells were performed on 4–5 μm paraffin-embedded sections with an *In situ* Apoptosis Detection Kit (R&D Systems, Minneapolis, MN, USA), according to the manufacturer's recommendations.

Metabolite measurements

Blood was drawn at 10 AM by cardiac puncture and exsanguination under anesthesia at the age of 4 mo and processed (21). Ascorbic acid in serum was measured with the ferric reducing ascorbate assay kit from BioVision Research Products (Mountain View, CA, USA). Metabolite measurements were performed by Biocrates Life Sciences metabolomic services (Biocrates Life Sciences, Innsbruck, Austria). In brief, Biocrates' commercially available kit plates were used for quantification of amino acids, acylcarnitines, sphingomyelins, phosphatidylcholines, hexoses, and biogenic amines. The fully automated assay was based on phenylisothiocyanate derivatization in the presence of internal standards followed by flow injection analysis–tandem mass spectrometry (MS) (acylcarnitines, lipids, and hexose) and liquid chromatography (LC)/MS (amino acids, biogenic amines) with a 4000 QTrap mass spectrometer (AB Sciex, Darmstadt, Germany) with electrospray ionization. The experimental metabolomics measurement technique has been described in Illig *et al.* (22). Eicosanoids and other oxidized polyunsaturated fatty acids were extracted from samples with aqueous acetonitrile that contained deuterated internal standards. The metabolites were determined by LC-MS/MS with multiple-reaction monitoring in negative mode on a 4000 QTrap mass spectrometer with electrospray ionization. The LC-MS/MS method used for the analytical determination of eicosanoids has been published (23). Accuracy of the measurements was in the normal range of the method (deviations from target, ≤20%) for all analytes. In total, 203 different metabolites were measured. The metabolomics data set contains 21 aa, 19 biogenic amines, 1 hexose (H1), free carnitine (C0), 40 acylcarnitines (C*x:y*), hydroxylacylcarnitines [C(OH)*x:y*], and dicarboxylacylcarnitines (C*x:y*-DC), 15 sphingomyelins (SM*x:y*), *N*-hydroxylacyloylsphingosylphosphocholine [SM(OH)*x:y*], 77 phosphatidylcholines (PC), 14 *lyso*-phosphatidylcholines, and 17 eicosanoid acids and prostaglandins. Lipid side-chain composition is abbreviated as C*x:y*, where *x* denotes the number of carbons in the side chain and *y* the number of double bonds. For example, PC acyl-

alkyl (PC ea) C30:1 denotes an acyl-alkyl phosphatidylcholine with 30 carbons in the 2 fatty acid side chains and 1 double bond in one of them (22). The precise position of the double bonds and the distribution of the carbon atoms in different fatty acid side chains cannot be determined with this technology. Full biochemical names and raw data are provided in the Excel spreadsheets of Supplemental Data S1.

Cytokine measurements

The following cytokines were assessed in the serum (diluted 1:4) using the multiplex kit from Bio-Rad Laboratories (MD000000EL; Mississauga, ON, Canada): IL-15, IL-18, leukemia inhibitory factor, macrophage–colony-stimulating factor (M-CSF), monokine induced by γ-interferon (MIG), macrophage inflammatory protein (MIP)-2, platelet-derived growth factor-BB, VEGF, and fibroblast growth factor (FGF) basic. The following cytokines were assessed in the serum (diluted 1:4) using the Multiplex Kit from Bio-Rad Laboratories (MD60009RDPD): IL-1α, -1β, -2, -3, -4, -5, -6, -10, -12 (p40), -12 (p70), -13, and -17; katacalcin (KC); monocyte chemoattractant protein-1; MIP-1α and -1β; TNF-α; regulated on activation, normal T-cell–expressed and –secreted (RANTES); Eotaxin; granulocyte–colony-stimulating factor (G-CSF); granulocyte-macrophage–colony-stimulating factor (GM-CSF); and IFN-γ. The metabolic hormones C-peptide 2, gastric inhibitory polypeptide, leptin, and resistin were assessed in serum with the Milliplex Mouse Metabolic Magnetic Bead Panel (MMHMAG-44K) from MilliporeSigma (Billerica, MA, USA). The following cardiovascular risk factors were assessed in the serum (diluted 1:20) using the Milliplex Mouse CVD Panel 1 Kit from MilliporeSigma (MCVD1MAG-77K): soluble E- and P-selectin, intercellular adhesion molecule-1, platelet endothelial cell adhesion molecule-1, pro-matrix metalloproteinase (MMP)-9, thrombomodulin, and total plasminogen activation inhibitor (PAI)-1. Full biologic names and raw data are provided in the Supplemental Table S1. All measurements were performed on a Bio-Plex 200 System (Bio-Plex Manager Software v.6.0; Bio-Rad Laboratories.)

Microcomputerized tomography analysis of trabecular and cortical bone

High-resolution images of femurs were acquired by using a Scanco VivaCT 40 (Bruettisellen, Switzerland). The femurs were scanned with the source voltage of 55 kV, a source current of 142 μA, and an isotropic voxel size of 10.5 μm. After the scanning, 3D microstructural image data were reconstructed and structural indices were calculated with Scanco μCT V6.1 Software. The number of femurs from 4-mo-old mice analyzed by micro-CT analysis were n = 8 WT, n = 10 $Wrn^{\Delta hel/\Delta hel}$, n = 10 $Gulo^{-/-}$, n = 12 $Wrn^{\Delta hel/\Delta hel}/Gulo^{-/-}$ mice with supplemental 0.01% ascorbate, and n = 8 $Wrn^{\Delta hel/\Delta hel}/Gulo^{-/-}$ mice treated with supplemental 0.4% ascorbate.

The area for the trabecular analysis started 57.5 μm proximal from the growth plate at the distal end of the femur and extended proximally 1050 μm toward the femoral head. The region of interest (ROI) for trabecular microarchitectural variables was defined by manually outlining the bone within the endocortical margins, allowing a few voxels between the ROI and the endocortical margin (24). An upper threshold of 1000 Hounsfield units and a lower threshold of 220 Hounsfield units were used to delineate each pixel as bone or nonbone. Representative 2-dimensional cross-sectional images for each genotype within the young and aged groups are shown in gray scale. Trabecular bone volume per total volume (%), mean trabecular thickness (mm), mean trabecular number (1/mm), and mean trabecular separation (mm) indices were computed.

Fractionation procedures for tissues

Total liver protein extracts were prepared as described elsewhere (21). Total endoplasmic reticulum (ER) fractions from mouse livers were obtained with an ER Enrichment Assay Kit (Novus Biologicals, Burlington, ON, Canada) according to the manufacturer's protocol. Enriched ER pellets were resuspended in suspension buffer containing phosphatase inhibitor cocktail (PhosStop Easy Pack) from Roche Applied Sciences (Indianapolis, IN, USA).

Western blot analyses

Western blot analyses were performed as described in Aumailley *et al.* (21). When indicated, immunoblots were probed with the following antibodies: rabbit polyclonal antibodies raised against the eukaryotic translation initiation factor 2-α kinase 3 [anti-PERK (H300): sc-13073]; eukaryotic translation factor 2-α [anti-eIF2α (FL-315): sc-11386]; phosphorylated eukaryotic translation factor 2-α [anti-p-eIF2α (Ser 52): sc-101670]; heat shock cognate (HSC) 70 kDa protein [anti-HSP70/HSC70 (H300): sc-33575]; cAMP-dependent transcription factor (ATF)-4 [anti-CREB-2 (C-20): sc-200]; ubiquitin [anti-Ub (FL-76): sc-9133]; homocysteine-inducible, endoplasmic reticulum stress-inducible, ubiquitin-like domain member-1 [anti-HERP (H-59): sc-98669]; and Werner syndrome protein [anti-WRN (H-300): sc-5629] were from Santa Cruz Biotechnology (Dallas, TX, USA). A mouse mAb against ATF-6α [anti-ATF-6α (F-7): sc-166659] and C/EBP-homologous protein (CHOP) [anti-GADD153 (B-3): sc-7351] was from Santa Cruz Biotechnology; rabbit mAb against inositol-requiring kinase-1α [anti-inositol-requiring enzyme (IRE)-1 (14C10) 3294], protein disulfide isomerase [anti-protein disulfide isomerase (PDI) (C81H6) 3501] from Cell Signaling Technology (Beverly, MA, USA); a rabbit pAb against glucose-related protein-78 (anti-GRP78) from Proteintech (Chicago, IL, USA); a rabbit pAb against calreticulin (anti-calreticulin; ER marker ab39818) from Abcam (Cambridge, United Kingdom); and a mouse mAb against actin (A5441) from MilliporeSigma.

Reactive oxygen species measurements in liver tissues and ER fractions from mouse livers

Liver lysates in RIPA buffer [50 mM Tris-HCl (pH 7.5), 150 mM NaCl, 1% NP-40, 0.1% SDS, 0.5% sodium deoxycholate, 1 mM PMSF, and complete protease inhibitor cocktail (Roche Applied Science)] or ER enriched fractions from mouse livers were incubated with 10 µg/ml of the dye 2′-7′ dichlorofluorescein diacetate (DCFA) (MilliporeSigma) for 1 h at 37°C. As controls, RIPA buffer or ER suspension buffer was also incubated with DCFA, and 100 µl (500 µg of liver proteins or 100 µg of ER fractions) of the samples was put into 96-well plates. Fluorescence was measured with a SpectraMax i3x Multi-Mode microplate reader (Molecular Devices, Sunnyvale, CA, USA). The excitation and emission wavelengths used were 485 and 527 nm, respectively.

Protein sulfhydryl measurements in total liver tissues

Weighed liver tissues were homogenized on ice in 20 mM sodium phosphate buffer (pH 7.4) containing 140 mM potassium chloride. Samples were then incubated in lysis buffer for 30 min on a rotary device at 4°C. Protein sulfhydryls were measured by monitoring the reaction between free thiol groups on proteins (240 µg of liver proteins) and the colorimetric reagent 5,5′-dithio-*bis*-(2-nitrobenzoic acid) (DTNB; MilliporeSigma) (25, 26).

Statistical analysis

We used a 1-sided Fisher exact test for comparison between the mitochondrial mutation rates between all genotypes. A Student's *t* test was performed when indicated between different cohorts of mice. Data in graphs are presented ± SEM, and differences between groups were considered significant when $P < 0.05$. The identification of significantly different metabolites and cytokines was performed using the Kruskal-Wallis nonparametric test. Principal component analysis (PCA) and presentation of the results using heat maps were performed using R v.2.14 (*https://www.r-project.org/*). We considered events significant at $P < 0.01$. Heat maps were generated using Euclidian distance and complete agglomerative methods. One-way ANOVA followed by Tukey's honest significant difference test or Sidak's multiple-comparisons test for post-ANOVA pair-wise comparisons was performed for the morphologic studies and for the Western blot analyses. Differences were considered significant when $P < 0.05$.

RESULTS

Lifespan and body weight of $Wrn^{\Delta hel/\Delta hel}/Gulo^{-/-}$ mice treated with 0.01 and 0.4% ascorbate

$Gulo^{-/-}$ and $Wrn^{\Delta hel/\Delta hel}$ mice were crossed to generate $Wrn^{\Delta hel/\Delta hel}/Gulo^{-/-}$ mice to assess the role of ascorbate (vitamin C) on the lifespan of double-mutant homozygous mice. Littermates of all genotypes (males and females) were carefully followed throughout the years and scored for the occurrence of any sign of disease. Since WT and $Wrn^{\Delta hel/\Delta hel}$ mice synthesize their own ascorbate, they did not receive supplemental ascorbate in this study. The maximum lifespan of $Wrn^{\Delta hel/\Delta hel}$ and WT mice was 26 and 30 mo of age, respectively (**Fig. 1*A***). As $Gulo^{-/-}$ mice become rapidly ill without ascorbate, 0.01% of sodium ascorbate (w/v) was added to drinking water at weaning. Under these conditions, 50% of the $Gulo^{-/-}$ mice survived for at least the first 8 mo without any problem and were fertile. The oldest $Gulo^{-/-}$ animal died at the age of 16 mo. The $Wrn^{\Delta hel/\Delta hel}/Gulo^{-/-}$ mice treated with 0.01% ascorbate were smaller and sterile, became sick, and had to be humanely euthanized once they had lost more than 20% of their total body weight. The median lifespan of the $Wrn^{\Delta hel/\Delta hel}/Gulo^{-/-}$ mice was ~3 mo. The oldest $Wrn^{\Delta hel/\Delta hel}/Gulo^{-/-}$ animal died at the age of ~8 mo. The difference in lifespan between $Wrn^{\Delta hel/\Delta hel}/Gulo^{-/-}$ and $Gulo^{-/-}$ mice treated with 0.01% ascorbate was significant (log rank test; $P = 3.2 \times 10^{-12}$). When we supplemented drinking water with 0.4% ascorbate, 50% of the $Wrn^{\Delta hel/\Delta hel}/Gulo^{-/-}$ mice survived for at least the first 20 mo without any problem. The oldest $Wrn^{\Delta hel/\Delta hel}/Gulo^{-/-}$ mouse treated with 0.4% ascorbate was euthanized at the age of 27 mo as it became moribund. These mice exhibited splenomegaly, enlarged mesenteric lymph nodes, myeloid leukemias, or liver tumors. The difference in lifespan between $Wrn^{\Delta hel/\Delta hel}/Gulo^{-/-}$ mice treated with 0.01 and 0.4% ascorbate was significant (log rank test; $P = 4.4 \times 10^{-9}$). The lifespan of $Wrn^{\Delta hel/\Delta hel}/Gulo^{-/-}$ mice treated with 0.4% ascorbate was not significantly different compared with WT mice (log rank test; $P = 0.137$). However, the lifespan of $Wrn^{\Delta hel/\Delta hel}/Gulo^{-/-}$ mice treated with 0.4% ascorbate was also not significant to untreated $Wrn^{\Delta hel/\Delta hel}$ mice (log rank test; $P = 0.134$).

We next measured the amount of serum ascorbate in mice at 4 mo of age. The analysis also included 20-mo-old untreated WT mice. Four-mo-old $Gulo^{-/-}$ and $Wrn^{\Delta hel/\Delta hel}/Gulo^{-/-}$ mice treated with 0.01% of ascorbate since weaning had a significant decrease in serum ascorbate compared with untreated WT and $Wrn^{\Delta hel/\Delta hel}$ mice (Fig. 1*B*). Supplemental 0.4% ascorbate in

the drinking water increased serum ascorbate level in the $Wrn^{\Delta hel/\Delta hel}/Gulo^{-/-}$ mice to WT and $Wrn^{\Delta hel/\Delta hel}$ levels (Fig. 1*B*). ANOVA between groups of mice indicated a $P < 0.01$. The P values from the post-ANOVA Tukey test analysis are shown in the Supplemental Table S2, for the indicated comparisons between groups of mice. Finally, serum ascorbate levels in 4-mo-old mice correlated significantly with the maximum lifespan of each group of mice in our cohort (Fig. 1*C*).

Because patients with WS exhibit a lack of growth spurt during adolescence (27), we next followed the total body weight of male mice for the first 16 wk of life. On average the $Wrn^{\Delta hel/\Delta hel}/Gulo^{-/-}$ mice treated with 0.01% ascorbate were 15% smaller than the WT, $Wrn^{\Delta hel/\Delta hel}$ mice, and 0.01% ascorbate–treated $Gulo^{-/-}$ mice (Fig. 1*D*). There was no significant difference in body weight between WT, $Wrn^{\Delta hel/\Delta hel}$, and 0.01% ascorbate–treated $Gulo^{-/-}$ mice. When $Wrn^{\Delta hel/\Delta hel}/Gulo^{-/-}$ mice were treated with 0.4% ascorbate, total body weight was 17% higher than the WT mice at 16 wk of age (Fig. 1*E*). To determine whether $Wrn^{\Delta hel/\Delta hel}/Gulo^{-/-}$ mice were eating less with 0.01% ascorbate, we measured the daily food intake of our mice from each genotype for 1 wk at the age of 4 mo. As indicated in Fig. 1*F*, the $Wrn^{\Delta hel/\Delta hel}/Gulo^{-/-}$ mice treated with 0.01% ascorbate ate less than WT, $Wrn^{\Delta hel/\Delta hel}$, and 0.01% ascorbate–treated $Gulo^{-/-}$ mice. The food intake was similar to those 3 groups when $Wrn^{\Delta hel/\Delta hel}/Gulo^{-/-}$ mice received 0.4% ascorbate in the drinking water. We also measured the amount of water consumed by these mice for 1 wk at 4 mo of age. $Wrn^{\Delta hel/\Delta hel}/Gulo^{-/-}$ mice treated with 0.01% ascorbate drank less water every day than WT and $Wrn^{\Delta hel/\Delta hel}$ mice (Fig. 1*G*). When the water was supplemented with 0.4% ascorbate, $Wrn^{\Delta hel/\Delta hel}/Gulo^{-/-}$ mice drank significantly more water every day than WT mice (Fig. 1*G*). Finally, we determined that there was no significant correlation between food intake and total body weight or between water consumption and total body weight in our cohorts of mice. The Pearson's correlation coefficient r was 0.7395 ($P = 0.15$, not significant) for food intake *vs.* total body weight and 0.7031 ($P = 0.19$, not significant) for water consumption *vs.* total body weight. These results indicate that food intake and water consumption were not proportional to the different mean total body weight observed between the genotypes.

The heart, liver, spleen, and visceral fat were also weighed. As indicated in the Supplemental Fig. S1, the liver and heart did not show a significant difference between the different genotypes at 4 mo of age. There was no sign of cardiac or liver fibrosis in 4-mo-old $Wrn^{\Delta hel/\Delta hel}/Gulo^{-/-}$ mice treated with 0.01% ascorbate like the age-matched WT mice (data not shown). The spleen of 4-mo-old $Wrn^{\Delta hel/\Delta hel}$ mice was bigger than the spleen of WT mice. There was a tendency for the spleen to be larger in $Gulo^{-/-}$ and $Wrn^{\Delta hel/\Delta hel}/Gulo^{-/-}$ mice treated with 0.01% ascorbate than in WT mice of the same age (Supplemental Fig. S1). The spleen of $Wrn^{\Delta hel/\Delta hel}/Gulo^{-/-}$ mice treated with 0.4% ascorbate was significantly bigger than WT mice. The weight of visceral fat was significantly lower in $Wrn^{\Delta hel/\Delta hel}/Gulo^{-/-}$ mice treated with 0.01% ascorbate than in all the other groups of mice. $Wrn^{\Delta hel/\Delta hel}/Gulo^{-/-}$ mice treated with 0.4% ascorbate exhibited a significant increase in visceral fat weight compared with 0.01% ascorbate–treated $Wrn^{\Delta hel/\Delta hel}/Gulo^{-/-}$ mice, similar to weights in the other groups of mice (Supplemental Fig. S1).

Overall, our results indicate that $Wrn^{\Delta hel/\Delta hel}/Gulo^{-/-}$ mice had a reduced lifespan and were smaller than WT, $Wrn^{\Delta hel/\Delta hel}$, and 0.01% ascorbate–treated $Gulo^{-/-}$ mice when they were treated with a minimum of 0.01% ascorbate in drinking water. The supplementation of water with 0.4% ascorbate significantly increased the lifespan and the body weight of the $Wrn^{\Delta hel/\Delta hel}/Gulo^{-/-}$ mice.

Impact of 0.01 and 0.4% ascorbate supplementation on $Wrn^{\Delta hel/\Delta hel}/Gulo^{-/-}$ mouse fertility

Mating between $Wrn^{\Delta hel/\Delta hel}/Gulo^{-/-}$ males and females was unsuccessful in producing offspring when drinking water was supplemented with 0.01% ascorbate. However, when drinking water was supplemented with 0.4% ascorbate at weaning, adult $Wrn^{\Delta hel/\Delta hel}/Gulo^{-/-}$ mice produced offspring. Testes from each genotype were weighed at 4 mo of age and $Wrn^{\Delta hel/\Delta hel}/Gulo^{-/-}$ males exhibited a 25% decrease in size compared with WT, $Wrn^{\Delta hel/\Delta hel}$, and 0.01% ascorbate–treated $Gulo^{-/-}$ mice (**Fig. 2*A***). Note that the testes' wet weight did not correlate with the total body weight observed for the different genotypes at 4 mo of age (Pearson's correlation $r = 0.6493$; $P = 0.24$). The addition of 0.4% ascorbate in drinking water re-established the normal (WT) size of $Wrn^{\Delta hel/\Delta hel}/Gulo^{-/-}$ male testes. We performed histologic examination of the testes of $Wrn^{\Delta hel/\Delta hel}/Gulo^{-/-}$ males treated with 0.01% ascorbate and all anatomic structures (spermatids and Leydig and Sertoli cells) looked intact (Fig. 2*B*). Closer histologic examination of testicular sections at 4 mo of age by TUNEL assay revealed a major increase in overall cell death in $Wrn^{\Delta hel/\Delta hel}/Gulo^{-/-}$ mice compared with WT, $Wrn^{\Delta hel/\Delta hel}$, and 0.01% ascorbate–treated $Gulo^{-/-}$ mice. Cell death was significantly reduced in $Wrn^{\Delta hel/\Delta hel}/Gulo^{-/-}$ males treated with 0.4% ascorbate (Fig. 2*C, D*).

Finally, $Wrn^{\Delta hel/\Delta hel}/Gulo^{-/-}$ males treated with 0.01% ascorbate were crossed to WT females but did not produce vaginal plugs underlying other unknown physiologic problems during breeding. Adding 0.4% ascorbate in the drinking water reversed this breeding defect. $Wrn^{\Delta hel/\Delta hel}/Gulo^{-/-}$ females treated with 0.01% ascorbate were crossed to WT males. Although we could detect vaginal plugs, these females did not produce offspring. We performed histologic examination of the ovaries from $Wrn^{\Delta hel/\Delta hel}/Gulo^{-/-}$ adult females treated with 0.01% ascorbate and did not find any obvious anatomic abnormality (data not shown).

$Wrn^{\Delta hel/\Delta hel}/Gulo^{-/-}$ mice exhibit bone structure anomalies

Osteoporosis of the limbs has been described for patients with WS (27). We thus examined the bone structure of hind limbs in our mice. Upon tissue harvesting for histologic analysis, we found the hind limb femurs of $Wrn^{\Delta hel/\Delta hel}/Gulo^{-/-}$ mice to break more easily than those of WT mice. We performed micro-CT analysis of the femurs of 3-mo-old males from each genotype. **Figure 3*A*** shows representative images of the trabecular ROI for each of the genotypes. The bone volume decreased significantly in $Gulo^{-/-}$ and $Wrn^{\Delta hel/\Delta hel}/Gulo^{-/-}$ mice treated with 0.01% ascorbate compared with WT and $Wrn^{\Delta hel/\Delta hel}$ mice. Supplementation of 0.4% ascorbate to $Wrn^{\Delta hel/\Delta hel}/Gulo^{-/-}$ mice reversed bone volume to WT levels (Fig. 3*B*). The decrease in bone volume was accompanied by a significant decrease in trabecular number with a commensurate increase in trabecular separation in $Gulo^{-/-}$ and $Wrn^{\Delta hel/\Delta hel}/Gulo^{-/-}$ mice treated with 0.01% ascorbate (Fig. 3*C, D*). Trabecular thickness increased significantly in $Wrn^{\Delta hel/\Delta hel}$ and 0.01% ascorbate–treated $Wrn^{\Delta hel/\Delta hel}/Gulo^{-/-}$ mice (Fig. 3*E*) compared with WT and 0.01% ascorbate–treated $Gulo^{-/-}$ mice. All these phenotypes in $Wrn^{\Delta hel/\Delta hel}/Gulo^{-/-}$ mice were reversed by the supplementation of the drinking water with 0.4% ascorbate.

Cross-sectional images of $Wrn^{\Delta hel/\Delta hel}/Gulo^{-/-}$ femurs were overlaid onto WT, $Wrn^{\Delta hel/\Delta hel}$, and $Gulo^{-/-}$ mutant slices to illustrate bony abnormalities (Fig. 3*F–H*). There was an unusual distribution of trabecular bone (sequestration of bone toward the left quadrants) and misshapen cortical shell in $Wrn^{\Delta hel/\Delta hel}/Gulo^{-/-}$ mice treated with 0.01% ascorbate (Fig. 3*G*). These aberrant features in the $Wrn^{\Delta hel/\Delta hel}/Gulo^{-/-}$ mice were absent with 0.4% ascorbate (Fig. 3*H*).

Metabolomic profiling of mutant mice

As ascorbate has an impact not only on the lifespan of $Wrn^{\Delta hel/\Delta hel}/Gulo^{-/-}$ mice but also on their total visceral fat depots, we next examined 203 metabolites (including different lipid species) in the serum of the mouse cohorts described in Fig. 1*B* using a targeted MS approach. The serum metabolite concentrations in 6 males of each group are shown for all the metabolites in Supplemental Data S1. To identify the metabolites significantly altered between mouse cohorts, a nonparametric Kruskal-Wallis test was applied to the Supplemental Data S1. A summary of the metabolites significantly altered ($P < 0.01$) in at least 1 of the cohorts is given in a form of a heat map in **Fig. 4**. Changes were indicated as a *z*-score value for each metabolite in the serum of each animal. The heat map revealed 104 metabolites that significantly differed between groups (Fig. 4). These included 52 phosphatidylcholines, 6 lysophosphatidylcholines, 21 acylcarnitines, 8 biogenic amines, 5 prostaglandins, 7 sphingomyelins, hexoses, and 4 aa. The dendrogram on top of the heat map indicated that the 4-mo-old $Wrn^{\Delta hel/\Delta hel}$ and the WT mice were clustered together. $Wrn^{\Delta hel/\Delta hel}/Gulo^{-/-}$ mice given 0.01% ascorbate in their drinking water formed a distinct group. $Wrn^{\Delta hel/\Delta hel}/Gulo^{-/-}$ mice with 0.4% ascorbate in their drinking water formed other clusters with the old WT mice. We further explored the metabolic profile of each group by employing an unsupervised PCA on all the 203 metabolites (PCA in **Fig. 5**). The WT and the $Wrn^{\Delta hel/\Delta hel}$ mice clustered together in the middle of the upper part of the graph. The $Wrn^{\Delta hel/\Delta hel}/Gulo^{-/-}$ mice treated with 0.01% ascorbate clustered in the lower left quadrant of the graph. The $Wrn^{\Delta hel/\Delta hel}/Gulo^{-/-}$ mice treated with 0.4% ascorbate formed a cluster with the old WT (20-mo-old) mice in the middle of the lower part of the graph. $Gulo^{-/-}$ mice treated with 0.01% ascorbate clustered in the lower right quadrant of the graph. These results indicate that the overall metabolic profile of 4-mo-old $Wrn^{\Delta hel/\Delta hel}/Gulo^{-/-}$ mice treated with 0.01% ascorbate was very different from the other genotypes. The metabolic profile of $Wrn^{\Delta hel/\Delta hel}/Gulo^{-/-}$ mice treated with 0.4% ascorbate resembled the metabolic profile of 20-mo-old WT mice.

Inflammatory and cardiometabolic profiles of mutant mice

As metabolite disturbances can lead to an inflammatory response or changes in cardiovascular risk factors (22), we measured the levels of 42 cytokines/chemokines, metabolic hormones, and cardiovascular risk factors in the serum of our different mouse cohorts. Serum cytokine concentrations in 8 males of each group are shown in the Supplemental Table S1. To identify the cytokines significantly altered in either mouse groups, a nonparametric Kruskal-Wallis test was applied to the data. A summary of the cytokines significantly altered in at least one of the groups is given in a form of a heat map in **Fig. 6*A***. Changes were indicated as a *z*-score value for each cytokine in the serum of each animal. The dendrogram on top of the heat map indicated 2 major leaves. The young WT and the $Wrn^{\Delta hel/\Delta hel}$ mice tended to cluster together. All the $Wrn^{\Delta hel/\Delta hel}/Gulo^{-/-}$ mice treated with 0.01% ascorbate clustered together. The old WT, the $Gulo^{-/-}$ mice treated with 0.01% ascorbate, and the $Wrn^{\Delta hel/\Delta hel}/Gulo^{-/-}$ mice treated with 0.4% ascorbate were distributed unequally within the 2 major leaves of the dendrogram. To get a better picture for each group of mice, we performed an unsupervised PCA using data from all the cytokines (Fig. 6*B*). The PCA approach showed that all $Wrn^{\Delta hel/\Delta hel}/Gulo^{-/-}$ mice treated with 0.01% ascorbate were clustered in the lower left quadrant of the graph. The young (4 mo) WT mice were mainly clustered in the right quadrants of the graph with the $Wrn^{\Delta hel/\Delta hel}$ mice. The old (20 mo) WT mice were distributed in the upper quadrants and showed a large variability between individuals. The $Wrn^{\Delta hel/\Delta hel}/Gulo^{-/-}$ mice treated with 0.4% ascorbate were

also clustered in the upper quadrants of the graph and showed less variability between individuals. The *Gulo*$^{-/-}$ mice treated with 0.01% ascorbate were distributed in all 4 quadrants of the graph. To summarize the major finding of this PCA data, the serum cytokine profile of *Wrn*$^{\Delta hel/\Delta hel}$/*Gulo*$^{-/-}$ mice treated with 0.01% ascorbate was unique in our cohorts of mice and did not overlap with any other mouse groups.

The heat map revealed 9 cytokines or factors that significantly differed between groups (Fig. 6*A*). Graphs representing the levels of secreted factors in each group are shown in Supplemental Fig. S2. The most marked findings were a decreased in IL-12 (p70), G-CSF, MIP-1α, soluble E-selectin, and leptin in *Wrn*$^{\Delta hel/\Delta hel}$/*Gulo*$^{-/-}$ mice treated with 0.01% ascorbate than in WT mice. PAI-1 increased in *Wrn*$^{\Delta hel/\Delta hel}$/*Gulo*$^{-/-}$ mice treated with 0.01% ascorbate compared with WT mice. Treatment of *Wrn*$^{\Delta hel/\Delta hel}$/*Gulo*$^{-/-}$ mice with 0.4% ascorbate reversed the IL-12 (p70), G-CSF, MIP-1α, leptin, and PAI-1 phenotypes (Supplemental Fig. S2).

Ratios of specific metabolites indicate various pathway anomalies in *Wrn*$^{\Delta hel/\Delta hel}$/*Gulo*$^{-/-}$ mice

Figure 7 provides metabolite ratios that showed a significant difference between groups of mice. Methionine-sulfoxide (Met-SO) can be generated *via* a 2-electron–dependent mechanism and the Met-SO:Met ratio in the serum can be regarded as a marker of oxidative stress (28). As indicated in Fig. 7*A*, the Met-SO:Met ratio was significantly higher in *Wrn*$^{\Delta hel/\Delta hel}$/*Gulo*$^{-/-}$ mice treated with 0.01% ascorbate than in WT mice, indicating an increase oxidative stress in these mice. *Wrn*$^{\Delta hel/\Delta hel}$/*Gulo*$^{-/-}$ mice given supplemental 0.4% ascorbate only slightly, but not significantly, decreased this ratio.

Acylcarnitines are important molecules for mitochondrial function and lipid metabolism. As indicated in Fig. 4, 21 acylcarnitine species were significantly different among our different cohorts of mice. We examined the ratio of free carnitine over the sum of these 21 acylcarnitine species. As indicated in Fig. 7*B*, this ratio increased significantly in *Wrn*$^{\Delta hel/\Delta hel}$/*Gulo*$^{-/-}$ mice treated with 0.01% ascorbate compared with all the other groups of mice. *Wrn*$^{\Delta hel/\Delta hel}$/*Gulo*$^{-/-}$ mice given supplemental 0.4% ascorbate significantly reversed this ratio to WT. We also examined the ratio of saturated to unsaturated phosphatidylcholine species. We pooled the serum concentrations of saturated phosphatidylcholines and of unsaturated phosphatidylcholines to calculate a ratio. [For example, the concentrations of PC diacyl (PC aa) C26:0, PC aa C36:0, PC ae C36:0, PC ae C38:0, PC ae C40:0, and PC ae C42:0 that are significantly changed in our mouse cohorts based on Fig. 4 were summed to obtain the numerator of the ratio]. As indicated in Fig. 7*C*, the ratio of saturated:unsaturated phosphatidylcholines was not significantly different between groups, according to results of ANOVA. However, if we compared only the 0.01% ascorbate–treated *Wrn*$^{\Delta hel/\Delta hel}$/*Gulo*$^{-/-}$ mice with the WT mice, an unpaired Student *t* test showed a significant difference. *Wrn*$^{\Delta hel/\Delta hel}$/*Gulo*$^{-/-}$ mice given supplemental 0.4% ascorbate significantly reversed this ratio to WT levels.

Oxidative stress in the liver tissue of *Wrn*$^{\Delta hel/\Delta hel}$/*Gulo*$^{-/-}$ mice

We had found that the liver of *Wrn*$^{\Delta hel/\Delta hel}$ and *Gulo*$^{-/-}$ mice treated with low amounts of ascorbate (<0.01% in drinking water) exhibit an oxidative stress in the ER (11, 21, 29). The liver plays a pivotal role in nutrient, hormone, lipid, and metabolic waste product processing,

thereby maintaining body homeostasis (30). The liver ER is the normal location of ascorbate synthesis in mice (31). Furthermore, the active catalytic site of the membrane-associated Gulo enzyme is located in the ER lumen (32). We did not detect hepatic steatosis or significant difference in fat content between $Wrn^{\Delta hel/\Delta hel}/Gulo^{-/-}$ mice treated with 0.01% ascorbate compared with age-matched (4-mo-old) mice of the other groups (data not shown). However, we observed a significant increase in the mitochondrial DNA mutation rate in $Wrn^{\Delta hel/\Delta hel}/Gulo^{-/-}$ mice treated with 0.01% ascorbate compared with age-matched (4-mo-old) WT mice (**Table 1**). It was comparable to older (20-mo-old) WT mice. Treatment of $Wrn^{\Delta hel/\Delta hel}/Gulo^{-/-}$ mice with 0.4% ascorbate in drinking water decreased the mutation rate to young WT level (Table 1). The mutation rate in mitochondrial DNA of $Wrn^{\Delta hel/\Delta hel}$ and $Gulo^{-/-}$ mice treated with 0.01% ascorbate was not significantly different from that of age-matched WT mice. We next focused on reactive oxygen species (ROS) levels in the liver of $Wrn^{\Delta hel/\Delta hel}/Gulo^{-/-}$ mice and age-matched WT mice. We quantified ROS levels in total liver tissues of WT and $Wrn^{\Delta hel/\Delta hel}/Gulo^{-/-}$ mice treated with 0.01 or 0.4% ascorbate. ROS levels in total liver lysate from $Wrn^{\Delta hel/\Delta hel}/Gulo^{-/-}$ mice treated with 0.01% ascorbate increased significantly (~10%) compared with age-matched WT mice (**Fig. 8*A***). Treatment of $Wrn^{\Delta hel/\Delta hel}/Gulo^{-/-}$ mice with 0.4% ascorbate significantly decreased total ROS in the liver by ~16%.

We previously found that $Wrn^{\Delta hel/\Delta hel}$ mice exhibited a significant increase (~15%) in ROS levels in the ER fraction of their liver compared with WT mice (29). We next examined ROS levels in the ER fraction of liver from our $Wrn^{\Delta hel/\Delta hel}/Gulo^{-/-}$ mice. ROS level in the ER fraction of $Wrn^{\Delta hel/\Delta hel}/Gulo^{-/-}$ mice treated with 0.01% ascorbate increased significantly (2.2-fold) compared with that in age-matched WT mice (Fig. 8*B*). Treatment of $Wrn^{\Delta hel/\Delta hel}/Gulo^{-/-}$ mice with 0.4% ascorbate significantly decreased ER ROS to WT levels. These results indicate that 4-mo-old $Wrn^{\Delta hel/\Delta hel}/Gulo^{-/-}$ mice treated with 0.01% ascorbate exhibit greater oxidative ER stress levels than $Wrn^{\Delta hel/\Delta hel}$ mice (29). We thus examined different ER stress markers in our WT and $Wrn^{\Delta hel/\Delta hel}/Gulo^{-/-}$ mice. PERK and IRE1α were first analyzed by Western blot analysis in ER-enriched fractions (33). Calreticulin, a protein associated with the ER, was used as a loading control. The PERK protein level increased significantly in the liver ER of $Wrn^{\Delta hel/\Delta hel}/Gulo^{-/-}$ mice treated with 0.01% ascorbate compared with WT mice (**Fig. 9*A, B***). Treatment of $Wrn^{\Delta hel/\Delta hel}/Gulo^{-/-}$ mice with 0.4% ascorbate significantly decreased PERK to the WT level (Fig. 9*B*). IRE1α protein increased significantly in the liver ER enriched fraction of $Wrn^{\Delta hel/\Delta hel}/Gulo^{-/-}$ mice treated with 0.01 and 0.4% ascorbate compared with age-matched WT mice (Fig. 9*A, C*). There was no significant difference between the effects of the 0.01 and 0.4% ascorbate treatments in $Wrn^{\Delta hel/\Delta hel}/Gulo^{-/-}$ mice.

The PERK and IRE1α pathways are known to activate the transcription of CHOP (34). Since CHOP is not found in the ER, proteins from total liver lysates were analyzed by Western blot. β-actin was used as a loading control. There was only a tendency for CHOP to be increased in $Wrn^{\Delta hel/\Delta hel}/Gulo^{-/-}$ mice treated with 0.01% ascorbate compared with age-matched WT mice. By contrast, CHOP protein level increased significantly (~2-fold) in $Wrn^{\Delta hel/\Delta hel}/Gulo^{-/-}$ mice treated with 0.4% ascorbate compared with age-matched WT mice (Fig. 9*A, D*).

Upon ER stress, the ER membrane-associated ATF6 protein is cleaved into a subunit that translocates into the nucleus to activate the transcription of target genes (33). We thus examined the levels of full length and cleaved ATF6 in total liver extracts (Fig. 9*A, E, F*). There was only a tendency for the sum of full-length and cleaved ATF6 signals to be higher in the liver of $Wrn^{\Delta hel/\Delta hel}/Gulo^{-/-}$ mice treated with 0.01% ascorbate than in the liver of WT and $Wrn^{\Delta hel/\Delta hel}/Gulo^{-/-}$ mice treated with 0.4% ascorbate (Fig. 9*E*). However, when we calculated the ratio

of cleaved ATF6 over the sum of full-length and cleaved signals, the levels of cleaved ATF6 was higher in the $Wrn^{\Delta hel/\Delta hel}/Gulo^{-/-}$ mice treated with 0.01% ascorbate than in WT mice. The levels of cleaved ATF6 were even higher in the liver of $Wrn^{\Delta hel/\Delta hel}/Gulo^{-/-}$ mice treated with 0.4% ascorbate (Fig. 9*F*).

We have reported that the mutant Wrn protein ($Wrn^{\Delta hel}$) is mislocalized in the cytoplasm of $Wrn^{\Delta hel/\Delta hel}$ mice (11). Further microscopy analyses indicated a colocalization of $Wrn^{\Delta hel}$ proteins with the PDI. We examined the levels of PDI in our mouse cohort. As indicated in Fig. 9*A, G*, the levels of PDI increased significantly in $Wrn^{\Delta hel/\Delta hel}/Gulo^{-/-}$ mice treated with 0.01 and 0.4% compared with untreated WT mice. This PDI increase in the liver ER fraction of $Wrn^{\Delta hel/\Delta hel}/Gulo^{-/-}$ mice corresponded to the presence of $Wrn^{\Delta hel}$ protein in this ER fraction (Fig. 9*A, H*). No normal Wrn protein was detected in the ER fraction of WT mice. As previously found with $Wrn^{\Delta hel/\Delta hel}$ mice (29), the treatment of $Wrn^{\Delta hel/\Delta hel}/Gulo^{-/-}$ mice with 0.4% ascorbate in drinking water did not decrease the expression level of the mutant $Wrn^{\Delta hel}$ protein (Fig. 9*H*).

Total eIF2α, ATF4, glucose-regulated protein–78, and HSC70 protein levels were not different between WT and $Wrn^{\Delta hel/\Delta hel}/Gulo^{-/-}$ mice treated with different concentrations of ascorbate in drinking water (Supplemental Fig. S3). Phosphorylation of eIF2α was not significantly different between WT and ascorbate treated $Wrn^{\Delta hel/\Delta hel}/Gulo^{-/-}$ mice (Supplemental Fig. S3).

We also analyzed ATF4, CHOP, HSC70, and full-length and cleaved ATF6 protein levels in age-matched WT, $Wrn^{\Delta hel/\Delta hel}$, and 0.01% ascorbate–treated $Gulo^{-/-}$ mice, because it had not been examined in our other studies (11, 21, 29). There was no significant difference in CHOP, HSC70, or full-length and cleaved ATF6 protein levels between these groups of mice, according to ANOVA results (Supplemental Fig. S4). ATF4 was lower in $Wrn^{\Delta hel/\Delta hel}$, and 0.01% ascorbate–treated $Gulo^{-/-}$ mice compared with WT mice, but it was not significant according to ANOVA.

The ER-associated degradation pathway is increased in the liver tissue of $Wrn^{\Delta hel/\Delta hel}/Gulo^{-/-}$ mice

To eliminate misfolded proteins from the ER, cells rely on ubiquitin-proteasome–dependent ER-associated degradation (ERAD). Proteolysis of ERAD substrates by the proteasome requires their ubiquitylation and retrotranslocation from the ER to the cytoplasm (35). Homocysteine-inducible, endoplasmic reticulum stress-inducible, ubiquitin-like domain member (HERPUD)-1 protein facilitates ERAD. We thus examined the levels of HERPUD1 in the liver of WT and $Wrn^{\Delta hel/\Delta hel}/Gulo^{-/-}$ mice treated with 0.01 and 0.4% ascorbate. The HERPUD1 protein levels were significantly increased in the total lysates of $Wrn^{\Delta hel/\Delta hel}/Gulo^{-/-}$ mice treated with 0.01% ascorbate (Fig. 9*A, I*). Treating $Wrn^{\Delta hel/\Delta hel}/Gulo^{-/-}$ mice with 0.4% ascorbate significantly decreased HERPUD1 to WT levels. We next examined the levels of total protein ubiquitylation in the liver of WT and $Wrn^{\Delta hel/\Delta hel}/Gulo^{-/-}$ mice treated with 0.01 and 0.4% ascorbate by Western blots. Total β-actin was used as a loading control (Supplemental Fig. S5). As indicated in **Fig. 10*A***, total protein ubiquitylation levels increased significantly in the total lysates of $Wrn^{\Delta hel/\Delta hel}/Gulo^{-/-}$ mice treated with 0.01% ascorbate. Treating $Wrn^{\Delta hel/\Delta hel}/Gulo^{-/-}$ mice with 0.4% ascorbate significantly decreased total ubiquitylation to WT levels. In contrast, $Gulo^{-/-}$ mice treated with 0.01% ascorbate showed a significant decrease in HERPUD1 levels compared with age-matched WT mice (Supplemental Fig. S4*A, C*). The level of total protein ubiquitylation in the liver of $Gulo^{-/-}$ mice treated with 0.01% ascorbate tended to decrease compared

with that in WT mice but it was not significant according to ANOVA results (Supplemental Fig. S4*A, B*). HERPUD1 protein and total ubiquitylation levels were not different between untreated $Wrn^{\Delta hel/\Delta hel}$ and age-matched WT mice (Supplemental Fig. S4*A*–*C*). Overall, these results indicate that untreated $Wrn^{\Delta hel/\Delta hel}$ mice and $Gulo^{-/-}$ and $Wrn^{\Delta hel/\Delta hel}/Gulo^{-/-}$ mice treated with 0.01% ascorbate showed very different HERPUD1 and ubiquitylation levels in their liver.

Because we detected increased ROS in the liver tissues of $Wrn^{\Delta hel/\Delta hel}/Gulo^{-/-}$ mice treated with 0.01% ascorbate, we hypothesized that such ROS would react directly with the cysteine thiols of unfolded proteins or nascent peptides during protein synthesis to convert them to sulfenic acids (36). We thus extracted proteins from the liver tissues of WT and $Wrn^{\Delta hel/\Delta hel}/Gulo^{-/-}$ mice treated with 0.01 or 0.4% ascorbate and measured the levels of intact thiols on proteins with the DTNB reagent (26). The levels of intact thiols on proteins were significantly lower in WT and much lower in $Wrn^{\Delta hel/\Delta hel}/Gulo^{-/-}$ mice treated with 0.01% than in $Wrn^{\Delta hel/\Delta hel}/Gulo^{-/-}$ mice treated with 0.4% ascorbate (Fig. 10*B*) . Overall, these results indicate that the presence of the $Wrn^{\Delta hel}$ mutant protein in the liver of $Wrn^{\Delta hel/\Delta hel}/Gulo^{-/-}$ mice affected the levels of intact thiols on proteins in general, as well as the amount of ubiquitylated proteins. Treatment of $Wrn^{\Delta hel/\Delta hel}/Gulo^{-/-}$ mice with 0.4% ascorbate improved these phenotypes.

DISCUSSION

Mouse model

We possess in our laboratory a mouse line bearing a deletion of part of the helicase domain in the *WRN* gene ortholog (10). Such $Wrn^{\Delta hel/\Delta hel}$ mice develop metabolic abnormalities and age-related pathologies leading to a shorter mean lifespan compared with WT mice (10, 11, 29, 37). The phenotypes associated with these mice are improved with a 0.4% ascorbate treatment in drinking water (15, 19, 29). These results indicated that, even though, unlike humans (31), mice can synthesize their own ascorbate, additional ascorbate in the diet was necessary to improve the span of good health in this mouse model. To better evaluate the impact of different doses of ascorbate on the longevity and the pathophysiological phenotypes of our *Wrn* mutant mice, we crossed the $Wrn^{\Delta hel/\Delta hel}$ mice with a knockout mouse line that lacks the enzyme required for *de novo* ascorbate synthesis (encoded by the *Gulo* gene) (20).

As reported, $Gulo^{-/-}$ mice become rapidly sick without ascorbate in the drinking water but live up to ~16 mo when treated with 0.01% ascorbate and ~32 mo when treated with 0.4% ascorbate (21). In contrast, in our study, the maximum lifespan of $Wrn^{\Delta hel/\Delta hel}/Gulo^{-/-}$ mice treated with 0.01% ascorbate in drinking water was not longer than 8 mo (Fig. 1*A*). Thus, $Wrn^{\Delta hel/\Delta hel}$ mice unable to synthesize their own ascorbate showed a major decrease in their lifespan. The maximum lifespan of $Wrn^{\Delta hel/\Delta hel}/Gulo^{-/-}$ mice treated with 0.4% ascorbate in drinking water increased significantly, similar to that of the WT cohort ($P = 0.137$, log rank test). Although the maximum lifespan of $Wrn^{\Delta hel/\Delta hel}/Gulo^{-/-}$ mice treated with 0.4% ascorbate increased compared with that of $Wrn^{\Delta hel/\Delta hel}$ mice, the difference was not significant ($P = 0.134$, log rank test). This finding suggests that the beneficial effect of 0.4% ascorbate on lifespan is attributable to the pharmacological correction of the $Gulo^{-/-}$ mutation in our mouse model. However, it is possible that our $Wrn^{\Delta hel/\Delta hel}/Gulo^{-/-}$ cohort treated with 0.4% ascorbate was rather small ($n = 14$) and therefore did not provide enough statistical power to detect a significant difference when we compared $Wrn^{\Delta hel/\Delta hel}/Gulo^{-/-}$ mice treated with 0.4% ascorbate to untreated $Wrn^{\Delta hel/\Delta hel}$ mice. Nevertheless, the 0.4% ascorbate treatment significantly improved several

other abnormal phenotypes (such as body weight, fertility, or osteopenia) exacerbated by the $Wrn^{\Delta hel/\Delta hel}$ mutation on the $Gulo^{-/-}$ genetic background. Serum ascorbate levels in 4-mo-old mice correlated significantly with the maximum lifespan of each group of mice in our cohort. Also, our results indicated that supplementation of drinking water with 0.01% ascorbate was suboptimal for the span of good health of $Wrn^{\Delta hel/\Delta hel}/Gulo^{-/-}$ mice compared with $Gulo^{-/-}$ mice.

Unlike $Gulo^{-/-}$ mice, $Wrn^{\Delta hel/\Delta hel}/Gulo^{-/-}$ mice treated with 0.01% ascorbate were sterile, an effect encountered in some patients with WS (27). We could not detect specific anomalies with the ovaries of $Wrn^{\Delta hel/\Delta hel}/Gulo^{-/-}$ mice treated with 0.01% ascorbate. In contrast, the testicular weight of $Wrn^{\Delta hel/\Delta hel}/Gulo^{-/-}$ males treated with 0.01% ascorbate was significantly lower compared with that of $Gulo^{-/-}$, $Wrn^{\Delta hel/\Delta hel}$, and WT mice and this difference was independent of total body weight in our different mouse cohorts. The number of apoptotic figures revealed by the TUNEL assay indicated a significant increase in spermatogonia mortality in the testes of $Wrn^{\Delta hel/\Delta hel}/Gulo^{-/-}$ mice treated with 0.01% ascorbate. No information is available with regard to the prevalence of apoptotic cells in testes of patients with WS but it has been reported that aged men (70–89-yr-old) present a significant augmentation in apoptotic signals located in the nuclei of spermatogonia and primary spermatocytes compared with young men (24–40-yr-old) (38). The 0.4% ascorbate treatment reversed the testicular phenotype of $Wrn^{\Delta hel/\Delta hel}/Gulo^{-/-}$ mice and they were successful in producing offspring.

Because 66% of clinically confirmed WS patients develop osteoporosis at a young age (~35-yr of age) (39, 40), the bone structure in the limbs of mice was examined with a microcomputed tomography scan (24). The bone volume decreased significantly in $Gulo^{-/-}$ and $Wrn^{\Delta hel/\Delta hel}/Gulo^{-/-}$ mice treated with 0.01% ascorbate compared with WT and $Wrn^{\Delta hel/\Delta hel}$ mice. The decrease in bone volume was accompanied by a significant decrease in trabecular number with a commensurate increase in trabecular separation in $Gulo^{-/-}$ and $Wrn^{\Delta hel/\Delta hel}/Gulo^{-/-}$ mice treated with 0.01% ascorbate. Cross-sectional images of $Wrn^{\Delta hel/\Delta hel}/Gulo^{-/-}$ femurs overlaid onto WT, $Wrn^{\Delta hel/\Delta hel}$ and $Gulo^{-/-}$ mutant slices illustrated gross bony abnormalities, including an unusual distribution of trabecular bone and misshapen cortical shell in $Wrn^{\Delta hel/\Delta hel}/Gulo^{-/-}$ mice treated with 0.01% ascorbate compared with the other mouse cohorts including the $Gulo^{-/-}$ mice treated with 0.01% ascorbate (Fig. 3). Thus, the abnormal bone structure in $Wrn^{\Delta hel/\Delta hel}/Gulo^{-/-}$ mice was more severe than in the other mouse genotypes. Such aberrant osteopenic features of $Wrn^{\Delta hel/\Delta hel}/Gulo^{-/-}$ mice were absent upon treatment with 0.4% ascorbate in drinking water.

Body weight and metabolic profile of $Wrn^{\Delta hel/\Delta hel}/Gulo^{-/-}$ mice

A common feature among patients with WS is their short stature (27). $Wrn^{\Delta hel/\Delta hel}/Gulo^{-/-}$ mice treated with 0.01% ascorbate were smaller than all the other groups of mice, including untreated $Wrn^{\Delta hel/\Delta hel}$ and 0.01% ascorbate–treated $Gulo^{-/-}$ mice (Fig. 1*D*). However, contrary to what has been described for patients with WS (41), visceral fat weight was significantly lower in $Wrn^{\Delta hel/\Delta hel}/Gulo^{-/-}$ mice treated with 0.01% ascorbate (Supplemental Fig. S1). Concomitantly, our targeted MS analyses of serum metabolites revealed a decrease in the levels of several lysophosphatidylcholine and phosphatidylcholine lipid types and hexose molecules in $Wrn^{\Delta hel/\Delta hel}/Gulo^{-/-}$ mice treated with 0.01% ascorbate compared with levels in the other groups of mice. The serum leptin level in $Wrn^{\Delta hel/\Delta hel}/Gulo^{-/-}$ mice treated with 0.01% ascorbate was also severely lower than in the other groups of mice (Supplemental Fig. S2).

Leptin is an important hormone that regulates food intake according to body fat mass, and its secretion correlates with the size of adipose mass in mice (42–44). *Wrn*$^{\Delta hel/\Delta hel}$/*Gulo*$^{-/-}$ mice treated with 0.01% ascorbate ate less than the other groups of mice. Upon 0.4% ascorbate treatment, serum leptin level significantly increased and reached serum concentrations above 7000 pg/ml in *Wrn*$^{\Delta hel/\Delta hel}$/*Gulo*$^{-/-}$ mice. A study on serum leptin levels in *Gulo*$^{-/-}$ mice indicated no significant difference between the 0.01 and 0.4% treatments with concentrations reaching 4000–6000 pg/ml (21). Leptin serum levels are ~3000–4000 pg/ml in age-matched WT mice (this study and reference 21). In addition, *Gulo*$^{-/-}$ mice treated with 0.4% ascorbate do not drink or eat more than *Gulo*$^{-/-}$ mice treated with 0.01% ascorbate (21). These results indicate that *Wrn*$^{\Delta hel/\Delta hel}$/*Gulo*$^{-/-}$ mice treated with 0.01 or 0.4% ascorbate behave very differently from *Gulo*$^{-/-}$ mice.

In addition to lower levels of several lipid types in the serum, *Wrn*$^{\Delta hel/\Delta hel}$/*Gulo*$^{-/-}$ mice treated with 0.01% ascorbate exhibited a significant increase in the ratio of serum saturated and unsaturated lipids and the ratio of free carnitine:acylcarnitine compared with WT mice (Fig. 7*B, C*). Of note, dyslipidemia has been associated with 85% of patients with genetically confirmed WS (40). A decrease in unsaturated lipid species may lead to perturbation of cellular membrane fluidity with age (45). An abnormal increase in saturated lipids, in return, may contribute to the development of inflammatory and oxidative stress (46). Carnitine is necessary for the transport of fatty acids across the mitochondrial membrane for their catabolism during cycles of β-oxidation (47). It is possible that the lower levels of several acylcarnitine molecules (Fig. 4) are imputable to the overall decrease of several lipid types in the serum of *Wrn*$^{\Delta hel/\Delta hel}$/*Gulo*$^{-/-}$ mice treated with 0.01% ascorbate. This phenotype was not observed in all the other groups of mice.

As published for the *Gulo*$^{-/-}$ and *Wrn*$^{\Delta hel/\Delta hel}$ mice (21, 29), addition of 0.4% ascorbate to the drinking water also significantly improved the altered metabolic phenotypes observed in *Wrn*$^{\Delta hel/\Delta hel}$/*Gulo*$^{-/-}$ mice. The PCA clearly indicated that the metabolic profile of 4-mo-old *Wrn*$^{\Delta hel/\Delta hel}$/*Gulo*$^{-/-}$ mice treated with 0.01% ascorbate clustered together and did not overlap any other mouse group (Fig. 5). The metabolic profile of 4-mo-old *Wrn*$^{\Delta hel/\Delta hel}$/*Gulo*$^{-/-}$ mice treated with 0.4% ascorbate did not overlap the profile of 4-mo-old WT mice, but it did overlap the profile of 20-mo-old WT mice (Fig. 5). The reason for this overlap in metabolic profiles is unknown. We observed that *Wrn*$^{\Delta hel/\Delta hel}$/*Gulo*$^{-/-}$ mice treated with 0.4% ascorbate gained weight more rapidly than age-matched WT mice during the first 10–16 wk of life (Fig. 1*E*), which certainly affected their overall metabolic profile. In addition, the ratio of visceral fat weight to total body weight was similar between *Wrn*$^{\Delta hel/\Delta hel}$/*Gulo*$^{-/-}$ mice treated with 0.4% ascorbate and untreated 20-mo-old WT mice (Supplemental Fig. S1). Finally, the PCA indicated very little overlap between *Gulo*$^{-/-}$ and *Wrn*$^{\Delta hel/\Delta hel}$/*Gulo*$^{-/-}$ mice treated with 0.01% ascorbate. A recently published PCA showed that the metabolic profile of *Gulo*$^{-/-}$ mice treated with 0.4% ascorbate was similar to that of 4-mo-old *Gulo*$^{-/-}$ mice treated with 0.01% ascorbate and did not overlap the profile of age-matched untreated WT mice (21) and thus would not overlap that of 20-mo-old WT mice. Future longitudinal studies on the metabolic profiles of these mice will provide a more complete picture of what is happening to these different mouse cohorts with age.

Cytokinome profile of *Wrn*$^{\Delta hel/\Delta hel}$/*Gulo*$^{-/-}$ mice

Metabolite disturbances can lead to an inflammatory response or changes in cardiovascular risk factors (22), and we therefore measured the levels of 42 cytokines/chemokines, hormones, and cardiovascular risk factors in the serum of our different mouse cohorts. The PCA clearly indicated that the profile of 4-mo-old $Wrn^{\Delta hel/\Delta hel}/Gulo^{-/-}$ mice treated with 0.01% ascorbate was clustered and did not significantly overlap that of the other mouse groups (Fig. 6*B*). In contrast to the metabolic profile, the cytokinome profile of 4-mo-old $Wrn^{\Delta hel/\Delta hel}/Gulo^{-/-}$ mice treated with 0.4% ascorbate was much closer to the profile of 4-mo-old WT mice than that of 20-mo-old WT mice.

When we examined each analyte, the most marked findings were a significant decrease in IL-12 (p70), G-CSF, MIP-1α, and E-selectin, as well as a significant increase in PAI-1 in $Wrn^{\Delta hel/\Delta hel}/Gulo^{-/-}$ mice treated with 0.01% ascorbate compared with WT mice. IL-12(p70) promotes the differentiation of type-1 helper T (Th1) cells, thereby supporting cellular immunity (48). It is naturally produced by dendritic cells, macrophages, and neutrophils. G-CSFs and M-CSFs are hematopoietic cytokines that stimulate the bone marrow to produce granulocytes and macrophages for release into the bloodstream (49–51). G-CSF is produced by the endothelium, macrophages, and several other immune cells. M-CSF is produced in the bone marrow and by endothelial cells, fibroblasts, osteoblasts, and smooth muscle cells (52). MIP-1α is produced by macrophages and acts as a chemoattractant to a variety of cells, including monocytes, T cells, B cells, and eosinophils (53). E-selectin plays an important role in recruiting leukocytes to sites of vascular injury and allows leukocytes to tightly bind to the endothelial surface (54). The observed decrease of these cytokines in $Wrn^{\Delta hel/\Delta hel}/Gulo^{-/-}$ mice treated with 0.01% ascorbate may underscore a dysfunction of part of the immune system which may be less efficient to respond to tissue damage. Notably, intracellular ascorbate concentration is important for the activity of macrophages (55). A thorough analysis of the immune cells from these mice is necessary to determine which biologic processes are affected by the accumulation of an abnormal Wrn mutant protein in such cell types.

PAI-1 is a serine protease inhibitor that functions as the principal inhibitor of tissue plasminogen and hence the physiologic breakdown of blood clots (56). It has been reported that a depletion of human WRN protein with small interference RNA molecules leads to an overexpression of PAI-1 in human fibroblasts (57). Similarly, we have found a significant increase in serum PAI-1 level in $Wrn^{\Delta hel/\Delta hel}$ mice (29). Moreover, the serum concentration of ascorbate seems to regulate the expression of PAI-1. Indeed, we have reported that $Gulo^{-/-}$ mice without ascorbate treatment exhibit high serum levels of PAI-1 that is decreased upon ascorbate treatment (21). In the present study, we also observed an increase in serum PAI-1 in $Gulo^{-/-}$ mice treated with 0.01% ascorbate compared with WT mice. More important, we observed an additive effect of the *Wrn* and *Gulo* mutations as PAI-1 levels were even higher in $Wrn^{\Delta hel/\Delta hel}/Gulo^{-/-}$ mice treated with 0.01% ascorbate than in WT mice. This phenotype was completely reversed by 0.4% ascorbate treatment. PAI-1 is present in increased levels in various disease states such as cardiovascular diseases (during the development of vessel wall damage) (58) and metabolic syndrome (59). In inflammatory conditions, PAI-1 is secreted by endothelial cells and appears to play a significant role in the progression to fibrosis (60, 61). We found in other work that we can detect an increase in this cardiovascular risk factor in young $Wrn^{\Delta hel/\Delta hel}$ mice before they exhibit cardiac fibrosis and valvular aortic stenosis (13, 37).

Oxidative stress in the ER fraction of $Wrn^{\Delta hel/\Delta hel}/Gulo^{-/-}$ mice

Oxidative stress has been implicated in a wide variety of degenerative processes and age-related diseases (62, 63). *Wrn*$^{\Delta hel/\Delta hel}$/*Gulo*$^{-/-}$ mice treated with 0.01% ascorbate showed a higher level of ROS in comparison with age-matched WT littermates (Fig. 8*A*). This result is similar to what we reported for the total liver of *Gulo*$^{-/-}$ mice treated with 0.01% ascorbate in drinking water (21). Moreover, we observed a significant increase in the ratio of Met-SO:Met in the serum of both *Wrn*$^{\Delta hel/\Delta hel}$/*Gulo*$^{-/-}$ and *Gulo*$^{-/-}$ mice treated with 0.01% ascorbate compared with that in WT mice (Fig. 7*A*). The ratio of serum Met-SO:Met is known increase in several pathologic and inflammatory processes (28, 64). ROS levels or serum Met-SO:Met ratio did not increase in total liver extract of *Wrn*$^{\Delta hel/\Delta hel}$ mice compared with age-matched WT mice, as reported (29). *A priori*, these results indicated that the levels of oxidative stress in serum and total liver extracts of *Wrn*$^{\Delta hel/\Delta hel}$/*Gulo*$^{-/-}$ and *Gulo*$^{-/-}$ mice treated with 0.01% ascorbate would be similar. However, when we examined the mutation rate of mitochondrial DNA in our different mouse cohorts at 4 mo of age, oxidative stress was significantly higher only in *Wrn*$^{\Delta hel/\Delta hel}$/*Gulo*$^{-/-}$ mice treated with 0.01% ascorbate (Table 1). This mitochondrial DNA mutation rate was decreased by 0.4% ascorbate treatment to the WT level, as were the ROS levels in total liver. Ascorbate is believed to be used predominantly as an antioxidant in mitochondria (65), suggesting a more severe shortage of ascorbate in the mitochondria of *Wrn*$^{\Delta hel/\Delta hel}$/*Gulo*$^{-/-}$ mice treated with 0.01% ascorbate compared with *Gulo*$^{-/-}$ mice treated with 0.01% ascorbate.

Another significant difference between *Wrn*$^{\Delta hel/\Delta hel}$/*Gulo*$^{-/-}$ mice treated with 0.01% ascorbate and all the other mouse genotypes was found in the ER stress response. ROS levels in ER enriched fractions from the liver of 0.01% ascorbate treated *Wrn*$^{\Delta hel/\Delta hel}$/*Gulo*$^{-/-}$ mice was approximately twice the levels found in age-matched WT mice (Fig. 8*B*). We have reported that *Wrn*$^{\Delta hel/\Delta hel}$ mice exhibit a 20% increase in ROS levels in the liver ER enriched fractions compared with age-matched WT mice (29). The ER is the main site for the synthesis and folding of around one-third of the total proteome of a cell (66). Proper folding of nascent protein in the ER requires an oxidant environment. However, too much ROS in the ER may cause irreversible modifications to nascent proteins that are unable to fold correctly (67). The thiol-SH side chain of cysteine is susceptible to reaction with ROS, giving rise to a range of oxidative post-translational modifications that can affect the formation of disulfide bonds within or between peptide chains (64, 68). With the use of the Ellman reagent, we recorded a significant increase in total thiol content in the liver lysates of *Wrn*$^{\Delta hel/\Delta hel}$/*Gulo*$^{-/-}$ mice treated with 0.4% ascorbate compared with *Wrn*$^{\Delta hel/\Delta hel}$/*Gulo*$^{-/-}$ mice treated with 0.01% ascorbate.

The 3 branches of the ER response pathways were significantly activated in *Wrn*$^{\Delta hel/\Delta hel}$/*Gulo*$^{-/-}$ mice treated with 0.01% ascorbate compared with age-matched WT mice (Fig. 9). More specifically, cleaved ATF6 signal was increased, and total protein levels of PERK and IRE1α were increased. This finding is different from what we had reported for *Wrn*$^{\Delta hel/\Delta hel}$ and *Gulo*$^{-/-}$ mice. We had observed a significant increase in total IRE1α protein levels only in *Wrn*$^{\Delta hel/\Delta hel}$ mice compared with age-matched WT mice (11) and a significant increase in total PERK protein level in *Gulo*$^{-/-}$ mice treated with 0.01% ascorbate (21). These results indicate that oxidative stress is more severe in the hepatic ER of *Wrn*$^{\Delta hel/\Delta hel}$/*Gulo*$^{-/-}$ mice treated with 0.01% ascorbate than in *Wrn*$^{\Delta hel/\Delta hel}$ or *Gulo*$^{-/-}$ mice so treated.

Unfolded or damaged proteins can be targeted to the proteasome for degradation *via* ubiquitylation (69). HERPUD1 is an ER membrane protein that facilitates the degradation of ubiquitylated proteins through ERAD (35, 70). Total ubiquitylated proteins and HERPUD1 expression levels increased significantly in *Wrn*$^{\Delta hel/\Delta hel}$/*Gulo*$^{-/-}$ mice treated with 0.01% ascorbate com-

pared with age-matched WT mice. Upon 0.4% ascorbate treatment, HERPUD1 and total ubiquitylated protein levels normalized to the WT level. In parallel, the total PERK protein level was reversed to WT level upon 0.4% ascorbate treatment in the liver of $Wrn^{\Delta hel/\Delta hel}/Gulo^{-/-}$ mice. Notably, HERPUD1 expression is regulated by the PERK-dependent pathway during ER stress (71). In contrast, the levels of cleaved ATF6 and IRE1α proteins were still significantly higher in 0.4% ascorbate treated $Wrn^{\Delta hel/\Delta hel}/Gulo^{-/-}$ mice than WT mice (Fig. 9). Moreover, CHOP protein level increased significantly in 0.4% ascorbate treated $Wrn^{\Delta hel/\Delta hel}/Gulo^{-/-}$ mice. The CHOP response to the 0.4% ascorbate treatment in the liver of $Wrn^{\Delta hel/\Delta hel}/Gulo^{-/-}$ mice is intriguing as CHOP is known to suppress adipogenesis and limits expansion of fat mass *in vivo* in mice potentially allowing a longer survival time (72).

Like the $Wrn^{\Delta hel/\Delta hel}$ mice, $Wrn^{\Delta hel/\Delta hel}/Gulo^{-/-}$ mice synthesize a stable Wrn mutant protein that is also found in the ER enriched fractions of liver tissues (Fig. 9) (11). Addition of 0.4% ascorbate to the drinking water did not decrease this mutant $Wrn^{\Delta hel}$ protein that can potentially induce chronic ER stress in $Wrn^{\Delta hel/\Delta hel}/Gulo^{-/-}$ mice. The higher levels of cleaved ATF6 and IRE1α proteins in $Wrn^{\Delta hel/\Delta hel}/Gulo^{-/-}$ mice, even in the presence of 0.4% ascorbate in the drinking water, may represent a continuous chronic ER stress response. The constant high levels of cleaved ATF6 and IRE1α may allow $Wrn^{\Delta hel/\Delta hel}/Gulo^{-/-}$ mice to cope with this continuous stress. Similarly, $Wrn^{\Delta hel/\Delta hel}/Gulo^{-/-}$ mice exhibit a significant increased PDI protein levels in the ER enriched fractions during both 0.01 and 0.4% treatments. PDI plays a pivotal role in proper protein folding by disulfide bond formation (73, 74). Intracellular levels of ascorbate and its reduced form dehydroascorbate (DHA) are known to modulate the reduced status of the catalytic dithiol center of PDI, and hence its enzymatic activity (75). Ascorbate is an excellent electron donor and leads to DHA upon oxidation (65). However, the half-life of DHA is very short in the ER and can be reduced by PDI, oxidizing the active central dithiols of this enzyme. Oxidized PDI, in return, reacts with reduced substrate proteins yielding protein disulfides and finally a decrease in proper protein folding. Catalytically active PDI is regenerated in this last step (65). Alternatively, DHA can rapidly react with dithiols in unfolded or partially folded proteins in a PDI-independent manner (65). Thus, the greater availability of ascorbate in drinking water would ultimately improve PDI reactions and proper disulfide bonding of nascent peptides during protein synthesis in $Wrn^{\Delta hel/\Delta hel}/Gulo^{-/-}$ mice. Overall, the elevated mitochondrial DNA mutation rate, the increased ROS in the ER enriched fraction, the major chronic ER stress, the activation of the ERAD pathway, and the very low level of serum ascorbate in $Wrn^{\Delta hel/\Delta hel}/Gulo^{-/-}$ mice given only 0.01% ascorbate in the drinking water are reminiscent of ascorbate compartmentation disease in these mice (65, 76). In our $Wrn^{\Delta hel/\Delta hel}/Gulo^{-/-}$ mouse model treated with 0.01% ascorbate, there is not enough ascorbate for proper function of the ER compartment, leading to a chronic ER stress response.

CONCLUSIONS

An important step in future studies is to find the optimal ascorbate doses that have the maximum positive impact on health. Unfortunately, high doses of ascorbate can have deleterious side effects. For example, ascorbate is continuously catabolized by oxidation to DHA. Major alterations in the ascorbate/DHA balance toward a more pro-oxidant state in different cellular organelles including the ER may negatively affect specific biochemical reactions and the redox status of the cells (65, 76). In addition, oxalate is a major end product of ascorbate in humans that can cause accumulation of calcium oxalate stones and nephrocalcinosis (76). Ascorbate is also a cofactor for many enzymes in the ER that are important for the synthesis of proteins of

the extracellular matrix, and it has an impact on the proliferation, maintenance, and differentiation of stem cells (76). A low level of ascorbate may lead to developmental defects in different tissues, whereas too much could push preneoplastic cells toward more aggressive metastatic cells (76). Thus, appropriate *in vivo* models are necessary to gain important insights into the molecular processes modulated by different supplementation levels of ascorbate. In the present study, we generated a unique mouse model for WS that, as in humans, relies entirely on a dietary source of ascorbate to survive. These $Wrn^{\Delta hel/\Delta hel}/Gulo^{-/-}$ mice exhibited a severe reduction in their lifespan, lower body weight, sterility, and osteopenia when treated with a suboptimal dose of ascorbate. The metabolic and cytokine profiles of $Wrn^{\Delta hel/\Delta hel}/Gulo^{-/-}$ mice treated with 0.01% ascorbate were unique and very different from those of WT, $Wrn^{\Delta hel/\Delta hel}$, and $Gulo^{-/-}$ mice. Even the serum ascorbate level was significantly reduced compared with $Gulo^{-/-}$ mice treated with 0.01% ascorbate in drinking water. Although the phenotypes of $Wrn^{\Delta hel/\Delta hel}/Gulo^{-/-}$ mice were greatly improved upon 0.4% ascorbate treatment, the metabolic profile was different from age-matched $Wrn^{\Delta hel/\Delta hel}$ and WT mice. Finally, the severe reduction of serum ascorbate in $Wrn^{\Delta hel/\Delta hel}/Gulo^{-/-}$ mice revealed a chronic oxidative stress in the ER and a permanent activation of all branches of the ER stress response pathways. In addition, markers associated with the ubiquitin-proteasome–dependent ER-associated degradation pathway were increased. Augmenting the dose of ascorbate to obtain optimal serum vitamin C concentration reversed the activation of this pathway to WT levels, indicating that the pathway is a potential therapeutic target in WS.

Supplementary Material

This article includes supplemental data. Please visit *http://www.fasebj.org* to obtain this information.

ACKNOWLEDGMENTS

This work was supported by funding from the Canadian Institutes of Health Research (to M.L. and A.M.), and by U.S. National Institutes of Health (NIH) National Institute on Aging Grant R01AG028873 (to R.J.P.). L.A. is a scholar from the Fondation du Centre Hospitalier Universitaire de Québec. The authors declare no conflicts of interest.

Glossary

ATF	cAMP-dependent transcription factor
CHOP	C/EBP-homologous protein
DCFA	2′-7′ dichlorofluorescein diacetate
DHA	dehydroascorbate
DTNB	5,5′-dithio-*bis*-(2-nitrobenzoic acid)
eIF2α	eukaryotic translation factor 2-α
ER	endoplasmic reticulum
ERAD	ER-associated degradation
G-CSF	granulocyte colony-stimulating factor
Gulo	gulonolactone oxidase gene
H&E	hematoxylin and eosin
HERPUD	homocysteine-inducible, endoplasmic reticulum stress-inducible, ubiquitin-like domain member
HSC	heat shock cognate
IRE	inositol-requiring enzyme
LC	liquid chromatography
M-CSF	macrophage–colony-stimulating factor
Met-SO	methionine-sulfoxide
MIP	macrophage inflammatory protein
MS	mass spectrometry

PAI	plasminogen activator inhibitor
PC	phosphatidylcholine
PCA	principal component analysis
PC aa	PC diacyl
PC ae	PC acyl-alkyl
PDI	protein disulfide isomerase
PERK	eukaryotic translation initiation factor 2-α kinase-3
ROI	region of interest
ROS	reactive oxygen species
Wrn	Werner syndrome RecQ-like helicase gene
WS	Werner syndrome
WT	wild type

Footnotes

This article includes supplemental data. Please visit http://www.fasebj.org to obtain this information.

AUTHOR CONTRIBUTIONS

L. Aumailley, E. R. Paquet, R. J. Pignolo, A. Marette, and M. Lebel designed the research; L. Aumailley, M. J. Dubois, T. A. Brennan, C. Garand, and E. R. Paquet performed the research; E. R. Paquet, R. J. Pignolo, A. Marette, and M. Lebel contributed new reagents and analytic tools; L. Aumailley, M. J. Dubois, T. A. Brennan, E. R. Paquet, R. J. Pignolo, and M. Lebel analyzed the data; L. Aumailley and M. Lebel wrote the paper; and L. Aumailley, M. J. Dubois, T. A. Brennan, E. R. Paquet, R. J. Pignolo, A. Marette, and M. Lebel contributed intellectually to the paper.

REFERENCES

1. Epstein C. J., Martin G. M., Schultz A. L., Motulsky A. G. (1966) Werner's syndrome a review of its symptomatology, natural history, pathologic features, genetics and relationship to the natural aging process. *Medicine (Baltimore)* 45, 177–221 https://doi.org/10.1097/00005792-196605000-00001 [PubMed: 5327241]

2. Salk D. (1982) Werner's syndrome: a review of recent research with an analysis of connective tissue metabolism, growth control of cultured cells, and chromosomal aberrations. *Hum. Genet.* 62, 1–5 https://doi.org/10.1007/BF00295598 [PubMed: 6759366]

3. Yu C. E., Oshima J., Fu Y. H., Wijsman E. M., Hisama F., Alisch R., Matthews S., Nakura J., Miki T., Ouais S., Martin G. M., Mulligan J., Schellenberg G. D. (1996) Positional cloning of the Werner's syndrome gene. *Science* 272, 258–262 https://doi.org/10.1126/science.272.5259.258 [PubMed: 8602509]

4. Ozgenc A., Loeb L. A. (2005) Current advances in unraveling the function of the Werner syndrome protein. *Mutat. Res.* 577, 237–251 https://doi.org/10.1016/j.mrfmmm.2005.03.020 [PubMed: 15946710]

5. Balajee A. S., Machwe A., May A., Gray M. D., Oshima J., Martin G. M., Nehlin J. O., Brosh R., Orren D. K., Bohr V. A. (1999) The Werner syndrome protein is involved in RNA polymerase II transcription. *Mol. Biol. Cell* 10, 2655–2668 https://doi.org/10.1091/mbc.10.8.2655 [PMCID: PMC25497] [PubMed: 10436020]

6. Cooper M. P., Machwe A., Orren D. K., Brosh R. M., Ramsden D., Bohr V. A. (2000) Ku complex interacts with and stimulates the Werner protein. *Genes Dev.* 14, 907–912 [PMCID: PMC316545] [PubMed: 10783163]

7. Shen J. C., Loeb L. A. (2000) The Werner syndrome gene: the molecular basis of RecQ helicase-deficiency diseases. *Trends Genet.* 16, 213–220 https://doi.org/10.1016/S0168-9525(99)01970-8 [PubMed: 10782115]

8. Saintigny Y., Makienko K., Swanson C., Emond M. J., Monnat R. J., Jr. (2002) Homologous recombination resolution defect in Werner syndrome. *Mol. Cell. Biol.* 22, 6971–6978 https://doi.org/10.1128/MCB.22.20.6971-6978.2002 [PMCID: PMC139822] [PubMed: 12242278]

9. Crabbe L., Verdun R. E., Haggblom C. I., Karlseder J. (2004) Defective telomere lagging strand synthesis in cells lacking WRN helicase activity. *Science* 306, 1951–1953 https://doi.org/10.1126/science.1103619 [PubMed: 15591207]

10. Lebel M., Leder P. (1998) A deletion within the murine Werner syndrome helicase induces sensitivity to inhibitors of topoisomerase and loss of cellular proliferative capacity. *Proc. Natl. Acad. Sci. USA* 95, 13097–13102 https://doi.org/10.1073/pnas.95.22.13097 [PMCID: PMC23722] [PubMed: 9789047]

11. Aumailley L., Garand C., Dubois M. J., Johnson F. B., Marette A., Lebel M. (2015) Metabolic and phenotypic differences between mice producing a Werner syndrome helicase mutant protein and Wrn null mice. *PLoS One* 10, e0140292 https://doi.org/10.1371/journal.pone.0140292 [PMCID: PMC4598085] [PubMed: 26447695]

12. Labbé A., Garand C., Cogger V. C., Paquet E. R., Desbiens M., Le Couteur D. G., Lebel M. (2011) Resveratrol improves insulin resistance hyperglycemia and hepatosteatosis but not hypertriglyceridemia, inflammation, and life span in a mouse model for Werner syndrome. *J. Gerontol. A Biol. Sci. Med. Sci.* 66, 264–278 https://doi.org/10.1093/gerona/glq184 [PubMed: 20974729]

13. Trapeaux J., Busseuil D., Shi Y., Nobari S., Shustik D., Mecteau M., El-Hamamsy I., Lebel M., Mongrain R., Rhéaume E., Tardif J. C. (2013) Improvement of aortic valve stenosis by ApoA-I mimetic therapy is associated with decreased aortic root and valve remodelling in mice. *Br. J. Pharmacol.* 169, 1587–1599 https://doi.org/10.1111/bph.12236 [PMCID: PMC3724114] [PubMed: 23638718]

14. Lebel M., Lavoie J., Gaudreault I., Bronsard M., Drouin R. (2003) Genetic cooperation between the Werner syndrome protein and poly(ADP-ribose) polymerase-1 in preventing chromatid breaks, complex chromosomal rearrangements, and cancer in mice. *Am. J. Pathol.* 162, 1559–1569 https://doi.org/10.1016/S0002-9440(10)64290-3 [PMCID: PMC1851180] [PubMed: 12707040]

15. Massip L., Garand C., Paquet E. R., Cogger V. C., O'Reilly J. N., Tworek L., Hatherell A., Taylor C. G., Thorin E., Zahradka P., Le Couteur D. G., Lebel M. (2010) Vitamin C restores healthy aging in a mouse model for Werner syndrome. *FASEB J.* 24, 158–172 https://doi.org/10.1096/fj.09-137133 [PMCID: PMC3712979] [PubMed: 19741171]

16. Pagano G., Zatterale A., Degan P., d'Ischia M., Kelly F. J., Pallardó F. V., Calzone R., Castello G., Dunster C., Giudice A., Kilinç Y., Lloret A., Manini P., Masella R., Vuttariello E., Warnau M. (2005) In vivo prooxidant state in Werner syndrome (WS): results from three WS patients and two WS heterozygotes. *Free Radic. Res.* 39, 529–533 https://doi.org/10.1080/10715760500092683 [PubMed: 16036329]

17. Deschênes F., Massip L., Garand C., Lebel M. (2005) In vivo misregulation of genes involved in apoptosis, development and oxidative stress in mice lacking both functional Werner syndrome protein and poly(ADP-ribose) polymerase-1. *Hum. Mol. Genet.* 14, 3293–3308 https://doi.org/10.1093/hmg/ddi362 [PubMed: 16195394]

18. Labbé A., Turaga R. V., Paquet E. R., Garand C., Lebel M. (2010) Expression profiling of mouse embryonic fibroblasts with a deletion in the helicase domain of the Werner syndrome gene homologue treated with hydrogen peroxide. *BMC Genomics* 11, 127 https://doi.org/10.1186/1471-2164-11-127 [PMCID: PMC2838845] [PubMed: 20175907]

19. Lebel M., Massip L., Garand C., Thorin E. (2010) Ascorbate improves metabolic abnormalities in Wrn mutant mice but not the free radical scavenger catechin. *Ann. N. Y. Acad. Sci.* 1197, 40–44 https://doi.org/10.1111/j.1749-6632.2010.05189.x [PMCID: PMC3693984] [PubMed: 20536831]

20. Maeda N., Hagihara H., Nakata Y., Hiller S., Wilder J., Reddick R. (2000) Aortic wall damage in mice unable to synthesize ascorbic acid. *Proc. Natl. Acad. Sci. USA* 97, 841–846 https://doi.org/10.1073/pnas.97.2.841 [PMCID: PMC15418] [PubMed: 10639167]

21. Aumailley L., Warren A., Garand C., Dubois M. J., Paquet E. R., Le Couteur D. G., Marette A., Cogger V. C., Lebel M. (2016) Vitamin C modulates the metabolic and cytokine profiles, alleviates hepatic endoplasmic reticulum stress, and increases the life span of Gulo−/− mice. *Aging (Albany N.Y.)* 8, 458–483 [PMCID: PMC4833140] [PubMed: 26922388]

22. Illig T., Gieger C., Zhai G., Römisch-Margl W., Wang-Sattler R., Prehn C., Altmaier E., Kastenmüller G., Kato B. S., Mewes H. W., Meitinger T., de Angelis M. H., Kronenberg F., Soranzo N., Wichmann H. E., Spector T. D., Adamski J., Suhre K. (2010) A genome-wide perspective of genetic variation in human metabolism. *Nat. Genet.* 42, 137–141 https://doi.org/10.1038/ng.507 [PMCID: PMC3773904] [PubMed: 20037589]

23. Unterwurzacher I., Koal T., Bonn G. K., Weinberger K. M., Ramsay S. L. (2008) Rapid sample preparation and simultaneous quantitation of prostaglandins and lipoxygenase derived fatty acid metabolites by liquid chromatography-mass spectrometry from small sample volumes. *Clin. Chem. Lab. Med.* 46, 1589–1597 https://doi.org/10.1515/CCLM.2008.323 [PubMed: 18842110]

24. Bouxsein M. L., Boyd S. K., Christiansen B. A., Guldberg R. E., Jepsen K. J., Müller R. (2010) Guidelines for assessment of bone microstructure in rodents using micro-computed tomography. *J. Bone Miner. Res.* 25, 1468–1486 https://doi.org/10.1002/jbmr.141 [PubMed: 20533309]

25. Harrison F. E., Meredith M. E., Dawes S. M., Saskowski J. L., May J. M. (2010) Low ascorbic acid and increased oxidative stress in gulo(−/−) mice during development. *Brain Res.* 1349, 143–152 https://doi.org/10.1016/j.brainres.2010.06.037 [PMCID: PMC2914834] [PubMed: 20599829]

26. Ellman G. L. (1959) Tissue sulfhydryl groups. *Arch. Biochem. Biophys.* 82, 70–77 https://doi.org/10.1016/0003-9861(59)90090-6 [PubMed: 13650640]

27. Oshima J., Sidorova J. M., Monnat R. J., Jr. (2017) Werner syndrome: clinical features, pathogenesis and potential therapeutic interventions. *Ageing Res. Rev.* 33, 105–114 https://doi.org/10.1016/j.arr.2016.03.002 [PMCID: PMC5025328] [PubMed: 26993153]

28. Mashima R., Nakanishi-Ueda T., Yamamoto Y. (2003) Simultaneous determination of methionine sulfoxide and methionine in blood plasma using gas chromatography-mass spectrometry. *Anal. Biochem.* 313, 28–33 https://doi.org/10.1016/S0003-2697(02)00537-7 [PubMed: 12576054]

29. Aumailley L., Dubois M. J., Garand C., Marette A., Lebel M. (2015) Impact of vitamin C on the cardiometabolic and inflammatory profiles of mice lacking a functional Werner syndrome protein helicase. *Exp. Gerontol.* 72, 192–203 https://doi.org/10.1016/j.exger.2015.10.012 [PubMed: 26521679]

30. Hilmer S. N., Cogger V. C., Fraser R., McLean A. J., Sullivan D., Le Couteur D. G. (2005) Age-related changes in the hepatic sinusoidal endothelium impede lipoprotein transfer in the rat. *Hepatology* 42, 1349–1354 https://doi.org/10.1002/hep.20937 [PubMed: 16317689]

31. Linster C. L., Van Schaftingen E. (2007) Vitamin C. Biosynthesis, recycling and degradation in mammals. *FEBS J.* 274, 1–22 https://doi.org/10.1111/j.1742-4658.2006.05607.x [PubMed: 17222174]

32. Puskás F., Braun L., Csala M., Kardon T., Marcolongo P., Benedetti A., Mandl J., Bánhegyi G. (1998) Gulonolactone oxidase activity-dependent intravesicular glutathione oxidation in rat liver microsomes. *FEBS Lett.* 430, 293–296 https://doi.org/10.1016/S0014-5793(98)00678-4 [PubMed: 9688558]

33. Hotamisligil G. S. (2010) Endoplasmic reticulum stress and the inflammatory basis of metabolic disease. *Cell* 140, 900–917 https://doi.org/10.1016/j.cell.2010.02.034 [PMCID: PMC2887297] [PubMed: 20303879]

34. Brown M. K., Naidoo N. (2012) The endoplasmic reticulum stress response in aging and age-related diseases. *Front. Physiol.* 3, 263 https://doi.org/10.3389/fphys.2012.00263 [PMCID: PMC3429039] [PubMed: 22934019]

35. Schulze A., Standera S., Buerger E., Kikkert M., van Voorden S., Wiertz E., Koning F., Kloetzel P. M., Seeger M. (2005) The ubiquitin-domain protein HERP forms a complex with components of the endoplasmic reticulum associated degradation pathway. *J. Mol. Biol.* 354, 1021–1027 https://doi.org/10.1016/j.jmb.2005.10.020 [PubMed: 16289116]

36. Zito E., Hansen H. G., Yeo G. S., Fujii J., Ron D. (2012) Endoplasmic reticulum thiol oxidase deficiency leads to ascorbic acid depletion and noncanonical scurvy in mice. *Mol. Cell* 48, 39–51 https://doi.org/10.1016/j.molcel.2012.08.010 [PMCID: PMC3473360] [PubMed: 22981861]

37. Massip L., Garand C., Turaga R. V., Deschênes F., Thorin E., Lebel M. (2006) Increased insulin, triglycerides, reactive oxygen species, and cardiac fibrosis in mice with a mutation in the helicase domain of the Werner syndrome gene homologue. *Exp. Gerontol.* 41, 157–168 https://doi.org/10.1016/j.exger.2005.10.011 [PubMed: 16330174]

38. Jiang H., Zhu W. J., Li J., Chen Q. J., Liang W. B., Gu Y. Q. (2014) Quantitative histological analysis and ultrastructure of the aging human testis. *Int. Urol. Nephrol.* 46, 879–885 https://doi.org/10.1007/s11255-013-0610-0 [PubMed: 24277275]

39. Hofer A. C., Tran R. T., Aziz O. Z., Wright W., Novelli G., Shay J., Lewis M. (2005) Shared phenotypes among segmental progeroid syndromes suggest underlying pathways of aging. *J. Gerontol. A Biol. Sci. Med. Sci.* 60, 10–20 https://doi.org/10.1093/gerona/60.1.10 [PubMed: 15741277]

40. Takemoto M., Mori S., Kuzuya M., Yoshimoto S., Shimamoto A., Igarashi M., Tanaka Y., Miki T., Yokote K. (2013) Diagnostic criteria for Werner syndrome based on Japanese nationwide epidemiological survey. *Geriatr. Gerontol. Int.* 13, 475–481 https://doi.org/10.1111/j.1447-0594.2012.00913.x [PubMed: 22817610]

41. Mori S., Murano S., Yokote K., Takemoto M., Asaumi S., Take A., Saito Y. (2001) Enhanced intra-abdominal visceral fat accumulation in patients with Werner's syndrome. *Int. J. Obes. Relat. Metab. Disord.* 25, 292–295 https://doi.org/10.1038/sj.ijo.0801529 [PubMed: 11410834]

42. Fantuzzi G., Faggioni R. (2000) Leptin in the regulation of immunity, inflammation, and hematopoiesis. *J. Leukoc. Biol.* 68, 437–446 [PubMed: 11037963]

43. Margetic S., Gazzola C., Pegg G. G., Hill R. A. (2002) Leptin: a review of its peripheral actions and interactions. *Int. J. Obes. Relat. Metab. Disord.* 26, 1407–1433 https://doi.org/10.1038/sj.ijo.0802142 [PubMed: 12439643]

44. Maffei M., Halaas J., Ravussin E., Pratley R. E., Lee G. H., Zhang Y., Fei H., Kim S., Lallone R., Ranganathan S., Kern P. A., Friedman J. M. (1995) Leptin levels in human and rodent: measurement of plasma leptin and ob RNA in obese and weight-reduced subjects. *Nat. Med.* 1, 1155–1161 https://doi.org/10.1038/nm1195-1155 [PubMed: 7584987]

45. Yehuda S., Rabinovitz S., Carasso R. L., Mostofsky D. I. (2002) The role of polyunsaturated fatty acids in restoring the aging neuronal membrane. *Neurobiol. Aging* 23, 843–853 https://doi.org/10.1016/S0197-4580(02)00074-X [PubMed: 12392789]

46. Kennedy A., Martinez K., Chuang C. C., LaPoint K., McIntosh M. (2009) Saturated fatty acid-mediated inflammation and insulin resistance in adipose tissue: mechanisms of action and implications. *J. Nutr.* 139, 1–4 https://doi.org/10.3945/jn.108.098269 [PubMed: 19056664]

47. Kompare M., Rizzo W. B. (2008) Mitochondrial fatty-acid oxidation disorders. *Semin. Pediatr. Neurol.* 15, 140–149 https://doi.org/10.1016/j.spen.2008.05.008 [PubMed: 18708005]

48. Suzuki K., Nakaji S., Kurakake S., Totsuka M., Sato K., Kuriyama T., Fujimoto H., Shibusawa K., Machida K., Sugawara K. (2003) Exhaustive exercise and type-1/type-2 cytokine balance with special focus on interleukin-12 p40/p70. *Exerc. Immunol. Rev.* 9, 48–57 [PubMed: 14686094]

49. Stanley E. R., Berg K. L., Einstein D. B., Lee P. S., Pixley F. J., Wang Y., Yeung Y. G. (1997) Biology and action of colony-stimulating factor-1. *Mol. Reprod. Dev.* 46, 4–10 https://doi.org/10.1002/(SICI)1098-2795(199701)46:1%3c4::AID-MRD2%3e3.0.CO;2-V [PubMed: 8981357]

50. Metcalf D. (1985) The granulocyte–macrophage colony-stimulating factors. *Science* 229, 16–22 https://doi.org/10.1126/science.2990035 [PubMed: 2990035]

51. D'Amario D., Leone A. M., Borovac J. A., Cannata F., Siracusano A., Niccoli G., Crea F. (2018) Granulocyte colony-stimulating factor for the treatment of cardiovascular diseases: an update with a critical appraisal. *Pharmacol. Res.* 127, 67–76 [PubMed: 28602846]

52. Hamilton J. A. (2008) Colony-stimulating factors in inflammation and autoimmunity. *Nat. Rev. Immunol.* 8, 533–544 https://doi.org/10.1038/nri2356 [PubMed: 18551128]

53. Cook D. N. (1996) The role of MIP-1 alpha in inflammation and hematopoiesis. *J. Leukoc. Biol.* 59, 61–66 https://doi.org/10.1002/jlb.59.1.61 [PubMed: 8558069]

54. Graves B. J., Crowther R. L., Chandran C., Rumberger J. M., Li S., Huang K. S., Presky D. H., Familletti P. C., Wolitzky B. A., Burns D. K. (1994) Insight into E-selectin/ligand interaction from the crystal structure and mutagenesis of the lec/EGF domains. *Nature* 367, 532–538 https://doi.org/10.1038/367532a0 [PubMed: 7509040]

55. Gieseg S. P., Leake D. S., Flavall E. M., Amit Z., Reid L., Yang Y. T. (2009) Macrophage antioxidant protection within atherosclerotic plaques. *Front. Biosci. (Landmark Ed.)* 14, 1230–1246 https://doi.org/10.2741/3305 [PubMed: 19273127]

56. Iwaki T., Urano T., Umemura K. (2012) PAI-1, progress in understanding the clinical problem and its aetiology. *Br. J. Haematol.* 157, 291–298 https://doi.org/10.1111/j.1365-2141.2012.09074.x [PubMed: 22360729]

57. Castro E., Oviedo-Rodríguez V., Angel-Chávez L. I. (2008) WRN polymorphisms affect expression levels of plasminogen activator inhibitor type 1 in cultured fibroblasts. *BMC Cardiovasc. Disord.* 8, 5 https://doi.org/10.1186/1471-2261-8-5 [PMCID: PMC2292137] [PubMed: 18312663]

58. Gils A., Declerck P. J. (2004) The structural basis for the pathophysiological relevance of PAI-I in cardiovascular diseases and the development of potential PAI-I inhibitors. *Thromb. Haemost.* 91, 425–437 [PubMed: 14983217]

59. Lasić D., Bevanda M., Bošnjak N., Uglešić B., Glavina T., Franić T. (2014) Metabolic syndrome and inflammation markers in patients with schizophrenia and recurrent depressive disorder. *Psychiatr. Danub.* 26, 214–219 [PubMed: 25191767]

60. Sadowski M., Ząbczyk M., Undas A. (2014) Coronary thrombus composition: links with inflammation, platelet and endothelial markers. *Atherosclerosis* 237, 555–561 https://doi.org/10.1016/j.atherosclerosis.2014.10.020 [PubMed: 25463088]

61. Samad F., Ruf W. (2013) Inflammation, obesity, and thrombosis. *Blood* 122, 3415–3422 https://doi.org/10.1182/blood-2013-05-427708 [PMCID: PMC3829115] [PubMed: 24092932]

62. Carrero D., Soria-Valles C., López-Otín C. (2016) Hallmarks of progeroid syndromes: lessons from mice and reprogrammed cells. *Dis. Model. Mech.* 9, 719–735 https://doi.org/10.1242/dmm.024711 [PMCID: PMC4958309] [PubMed: 27482812]

63. López-Otín C., Blasco M. A., Partridge L., Serrano M., Kroemer G. (2013) The hallmarks of aging. *Cell* 153, 1194–1217 https://doi.org/10.1016/j.cell.2013.05.039 [PMCID: PMC3836174] [PubMed: 23746838]

64. Korovila I., Hugo M., Castro J. P., Weber D., Höhn A., Grune T., Jung T. (2017) Proteostasis, oxidative stress and aging. *Redox Biol.* 13, 550–567 https://doi.org/10.1016/j.redox.2017.07.008 [PMCID: PMC5536880] [PubMed: 28763764]

65. Bánhegyi G., Benedetti A., Margittai E., Marcolongo P., Fulceri R., Németh C. E., Szarka A. (2014) Subcellular compartmentation of ascorbate and its variation in disease states. *Biochim. Biophys. Acta* 1843, 1909–1916 https://doi.org/10.1016/j.bbamcr.2014.05.016 [PubMed: 24907663]

66. Martínez G., Duran-Aniotz C., Cabral-Miranda F., Vivar J. P., Hetz C. (2017) Endoplasmic reticulum proteostasis impairment in aging. *Aging Cell* 16, 615–623 https://doi.org/10.1111/acel.12599 [PMCID: PMC5506418] [PubMed: 28436203]

67. Vincenz-Donnelly L., Hipp M. S. (2017) The endoplasmic reticulum: a hub of protein quality control in health and disease. *Free Radic. Biol. Med.* 108, 383–393 https://doi.org/10.1016/j.freeradbiomed.2017.03.031 [PubMed: 28363604]

68. Rudyk O., Eaton P. (2014) Biochemical methods for monitoring protein thiol redox states in biological systems. *Redox Biol.* 2, 803–813 https://doi.org/10.1016/j.redox.2014.06.005 [PMCID: PMC4085346] [PubMed: 25009782]

69. Lemus L., Goder V. (2014) Regulation of endoplasmic reticulum-associated protein degradation (ERAD) by ubiquitin. *Cells* 3, 824–847 https://doi.org/10.3390/cells3030824 [PMCID: PMC4197631] [PubMed: 25100021]

70. Quiroga C., Gatica D., Paredes F., Bravo R., Troncoso R., Pedrozo Z., Rodriguez A. E., Toro B., Chiong M., Vicencio J. M., Hetz C., Lavandero S. (2013) Herp depletion protects from protein aggregation by up-regulating autophagy. *Biochim. Biophys. Acta* 1833, 3295–3305 https://doi.org/10.1016/j.bbamcr.2013.09.006 [PubMed: 24120520]

71. Ma Y., Hendershot L. M. (2004) Herp is dually regulated by both the endoplasmic reticulum stress-specific branch of the unfolded protein response and a branch that is shared with other cellular stress pathways. *J. Biol. Chem.* 279, 13792–13799 https://doi.org/10.1074/jbc.M313724200 [PubMed: 14742429]

72. Han J., Murthy R., Wood B., Song B., Wang S., Sun B., Malhi H., Kaufman R. J. (2013) ER stress signalling through eIF2α and CHOP, but not IRE1α, attenuates adipogenesis in mice. *Diabetologia* 56, 911–924 https://doi.org/10.1007/s00125-012-2809-5 [PMCID: PMC3606029] [PubMed: 23314846]

73. Zeeshan H. M., Lee G. H., Kim H. R., Chae H. J. (2016) Endoplasmic reticulum stress and associated ROS. *Int. J. Mol. Sci.* 17, 327 https://doi.org/10.3390/ijms17030327 [PMCID: PMC4813189] [PubMed: 26950115]

74. Okumura M., Kadokura H., Inaba K. (2015) Structures and functions of protein disulfide isomerase family members involved in proteostasis in the endoplasmic reticulum. *Free Radic. Biol. Med.* 83, 314–322 https://doi.org/10.1016/j.freeradbiomed.2015.02.010 [PubMed: 25697777]

75. Szarka A., Lőrincz T. (2014) The role of ascorbate in protein folding. *Protoplasma* 251, 489–497 https://doi.org/10.1007/s00709-013-0560-5 [PubMed: 24150425]

76. D'Aniello C., Cermola F., Patriarca E. J., Minchiotti G. (2017) Vitamin C in stem cell biology: impact on extracellular matrix homeostasis and epigenetics. *Stem Cells Int.* 2017, 8936156 https://doi.org/10.1155/2017/8936156 [PMCID: PMC5415867] [PubMed: 28512473]

Figures and Tables

Figure 1

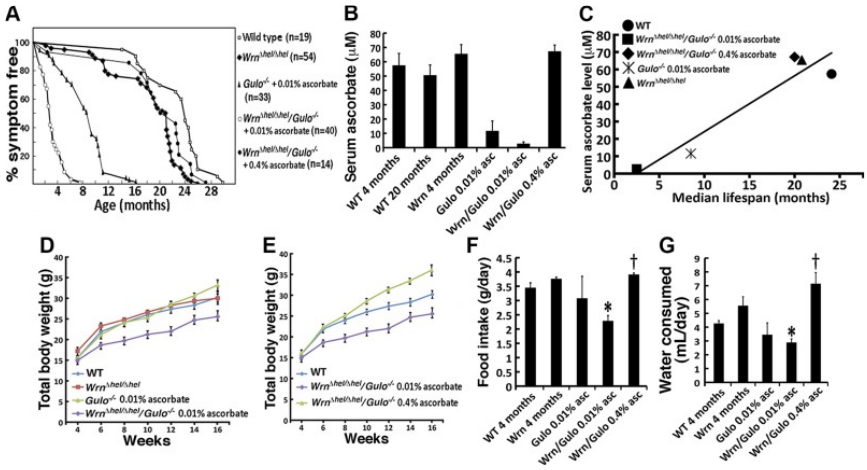

Effect of ascorbate on growth and lifespan of $Wrn^{\Delta hel/\Delta hel}/Gulo^{-/-}$ mice. *A*) Percentage of disease-free animals according to age for WT, $Wrn^{\Delta hel/\Delta hel}$, $Gulo^{-/-}$, and $Wrn^{\Delta hel/\Delta hel}/Gulo^{-/-}$ mice. *B*) Serum ascorbate levels in different groups of our mouse cohort (n = 6 per group). Bars represent SEM. Groups of mice are labeled in the graph: WT, wild type; Wrn, $Wrn^{\Delta hel/\Delta hel}$ mice; Gulo 0.01% asc: $Gulo^{-/-}$ mice given 0.01% supplemental ascorbate since weaning; Wrn/Gulo 0.01% asc, $Wrn^{\Delta hel/\Delta hel}/Gulo^{-/-}$ mice given 0.01% ascorbate since weaning; and Wrn/Gulo 0.4% asc, $Wrn^{\Delta hel/\Delta hel}/Gulo^{-/-}$ mice given 0.4% ascorbate since weaning. *C*) Correlation of serum ascorbate level and median lifespan. Graph showing the correlation between serum ascorbate level and median lifespan (Pearson's correlation coefficient $r = 0.942$; $P = 0.017$). *D*) Total body weight of the different groups of mice (n = 10) from the age of 4–16 wk. Bars represent SEM. *E*) Comparison of total body weight (age 4–16 wk) of untreated WT and $Wrn^{\Delta hel/\Delta hel}/Gulo^{-/-}$ mice treated with either 0.01 or 0.4% ascorbate (n = 10). Bars represent SEM. *F*) Food intake of mice (n = 3–6) at 4 mo of age. Bars represent SEM. Groups of mice are labeled as in panel *B*. $^{*}P < 0.044$ *vs.* WT mice; $^{\dagger}P < 0.011$ *vs.* $Wrn^{\Delta hel/\Delta hel}/Gulo^{-/-}$ mice given 0.01% supplemental ascorbate (by Tukey test). *G*) Water consumption of mice (n = 3–6) at 4 mo of age. Bars represent SEM. $^{*}P < 0.044$ *vs.* WT mice; $^{\dagger}P < 0.011$ *vs.* $Wrn^{\Delta hel/\Delta hel}/Gulo^{-/-}$ mice given 0.01% ascorbate (by Tukey test).

Figure 2

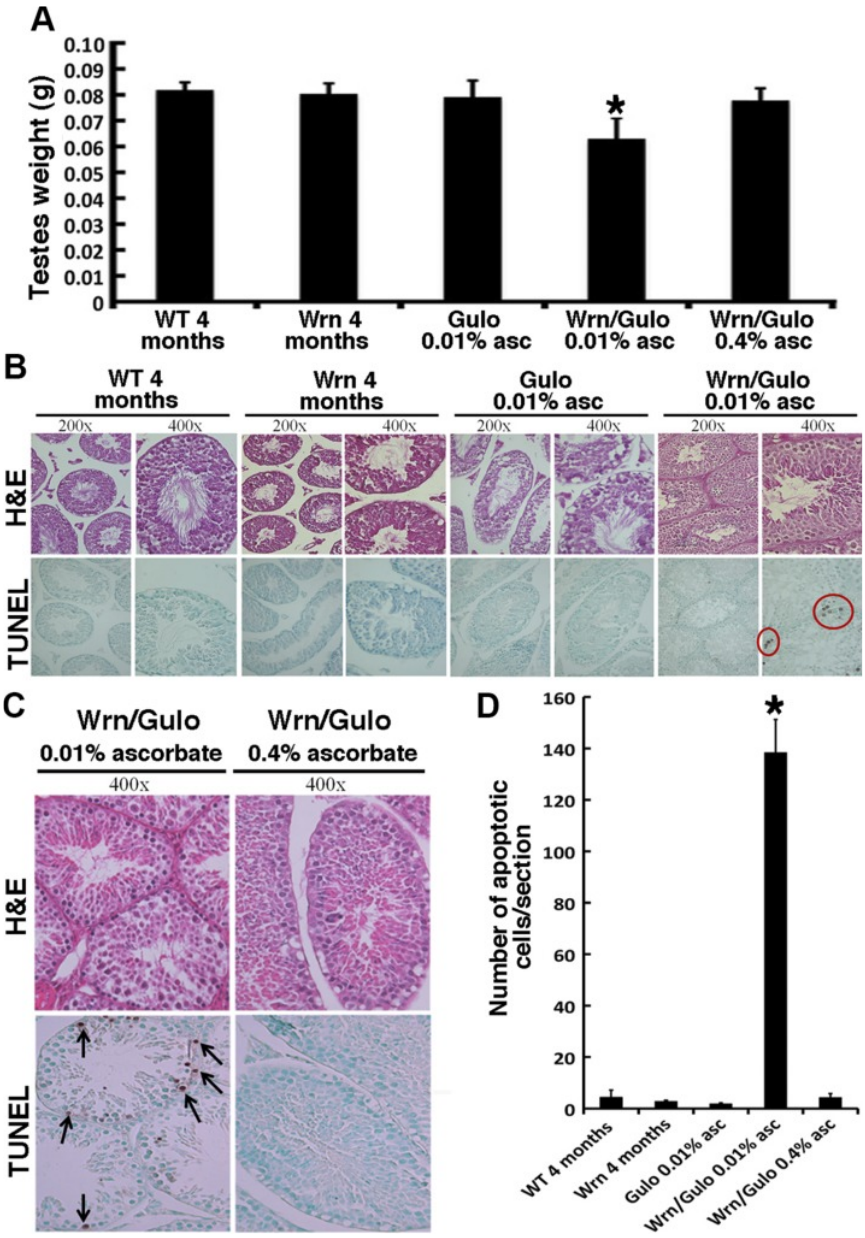

Effect of ascorbate on testicular morphology of $Wrn^{\Delta hel/\Delta hel}/Gulo^{-/-}$ mice. *A*) Testicular wet weight of mice (n = 10) at 4 mo of age. *P < 0.019 *vs.* all other groups of mice (by post-ANOVA Tukey test). *B*) H&E staining and TUNEL assay of seminiferous tubules of WT, $Wrn^{\Delta hel/\Delta hel}$, $Gulo^{-/-}$, and $Wrn^{\Delta hel/\Delta hel}/Gulo^{-/-}$ mice at 4 mo of age. Apoptotic cells are circled in red. *C*) H&E staining and TUNEL assay of seminiferous tubules of $Wrn^{\Delta hel/\Delta hel}/Gulo^{-/-}$ mice at 4 mo of age treated with 0.01 or 0.4% ascorbate. Apoptotic cells contain a brown precipitate (arrows). *D*) Average number of apoptotic cells per histologic section of testes from WT (n = 3), $Wrn^{\Delta hel/\Delta hel}$ (n = 4), $Gulo^{-/-}$ mice treated with 0.01% ascorbate (n = 4), $Wrn^{\Delta hel/\Delta hel}/Gulo^{-/-}$ mice treated with 0.01% ascorbate (n = 6), and $Wrn^{\Delta hel/\Delta hel}/Gulo^{-/-}$ mice treated with 0.4% ascorbate (n = 10) at 4 mo of age. *P < 0.001 *vs.* all other groups of mice (by Tukey test). Bars in graphs represent SEM. Groups of mice are labeled as in Fig. 1*B*.

Figure 3

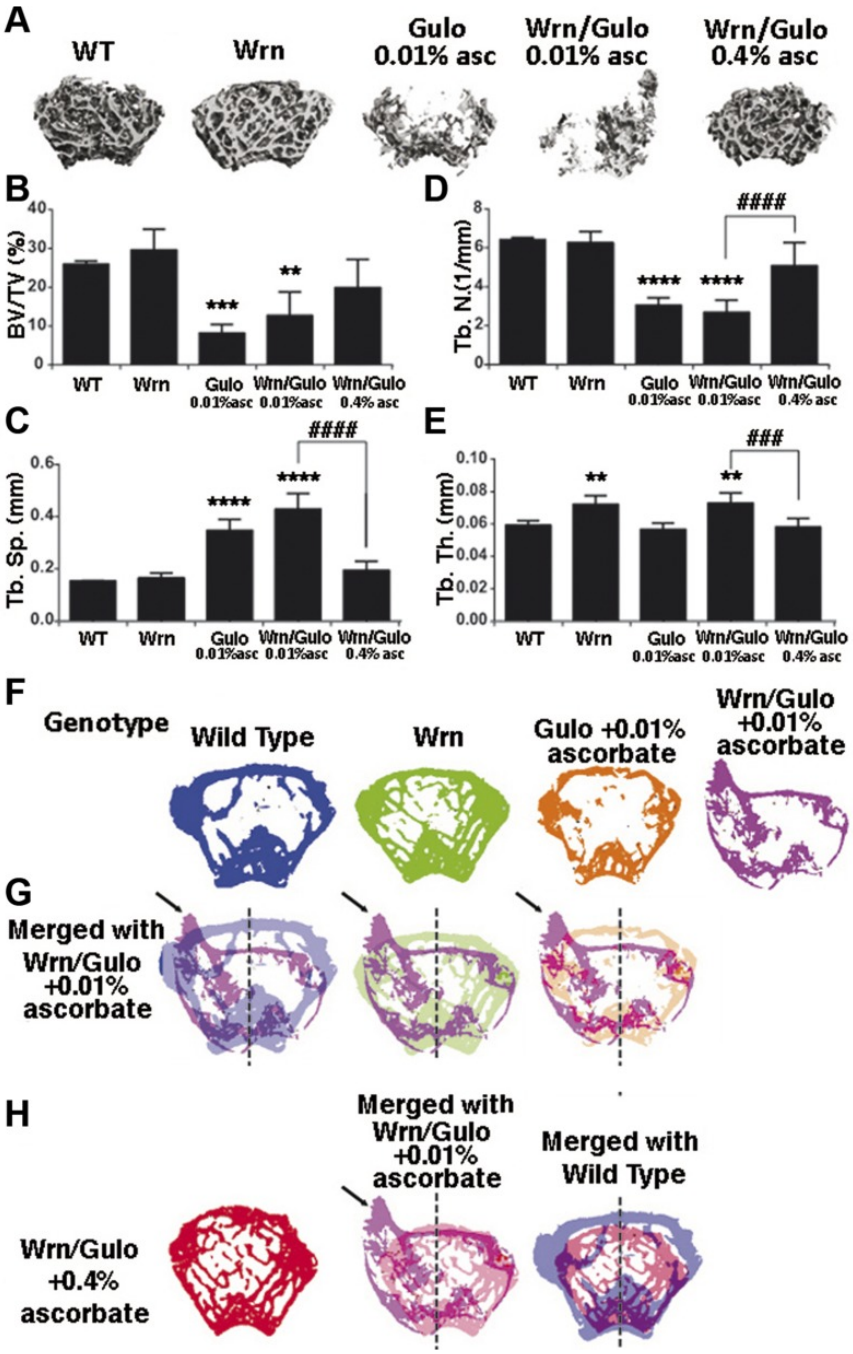

Impact of ascorbate on the hind limb bone structures of $Wrn^{\Delta hel/\Delta hel}/Gulo^{-/-}$ mice at 3 mo of age. *A*) Representative 3-dimensional reconstructions of the trabecular region of interest. *B*) Trabecular bone volume per total bone volume (%). *C*) Trabecular separation. *D*) Trabecular number. *E*) Trabecular thickness. *F*) Representative cross-sectional images of distal femurs from the indicated genotypes are shown. *G*) Cross-sectional images of femurs from $Wrn^{\Delta hel/\Delta hel}/Gulo^{-/-}$ mice treated with 0.01% ascorbate since weaning are overlaid onto WT, $Wrn^{\Delta hel/\Delta hel}$, and $Gulo^{-/-}$ mutant slices to illustrate bony abnormalities. Note the unusual distribution of trabecular bone (sequestration of bone toward the left quadrants), and misshapen cortical shell (arrow). *H*) Cross-sectional images of femurs from $Wrn^{\Delta hel/\Delta hel}/Gulo^{-/-}$ mice treated with 0.4% ascorbate overlaid onto femurs from $Wrn^{\Delta hel/\Delta hel}/Gulo^{-/-}$ mice treated with 0.01% ascorbate since weaning and femurs from untreated WT mice. Note that the aberrant features of the $Wrn^{\Delta hel/\Delta hel}/Gulo^{-/-}$ mutant are absent with the 0.4% ascorbate treatment. Labels in each panel: WT, wild type; Wrn, $Wrn^{\Delta hel/\Delta hel}$ mice; Gulo, $Gulo^{-/-}$ mice; Wrn/Gulo, $Wrn^{\Delta hel/\Delta hel}/Gulo^{-/-}$ mice. Bars in graphs represent SEM. $^{**}P > 0.01$; $^{***}P > 0.005$; $^{****}P > 0.0001$ *vs.* WT; $^{\#\#\#}P > 0.005$; $^{\#\#\#\#}P > 0.0001$ Wrn/Gulo 0.01% asc *vs.* Wrn/Gulo 0.01% asc (by 1-way ANOVA, with Sidak's multiple comparisons *post hoc* test).

Figure 4

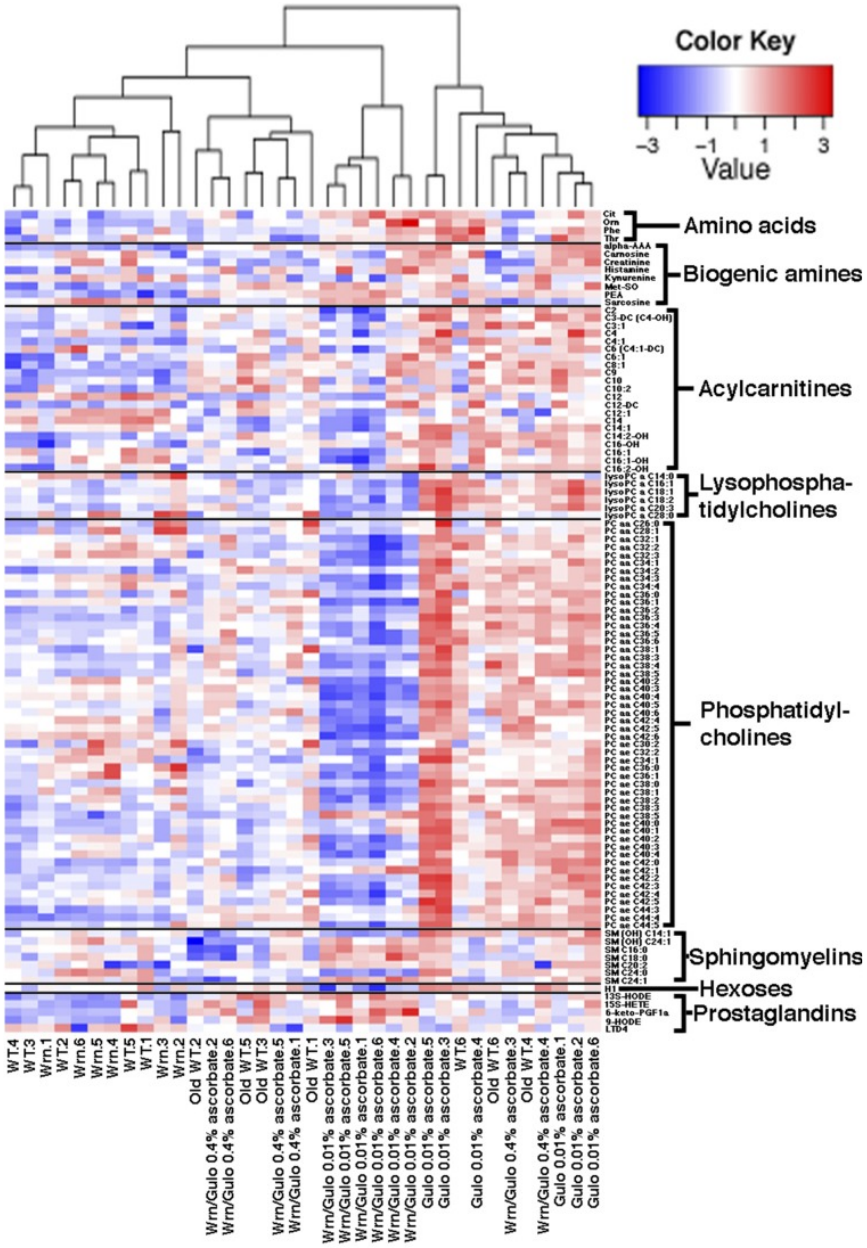

Heat map depicting the *z* score of the log base 10 in serum metabolites concentration (rows) between individual (columns) WT and mutant mice treated with different amounts of ascorbate. Columns are reordered by hierarchical clustering using the genotype and ascorbate treatments. Metabolites are grouped according to chemical classification. Young (4 mo) WT mice are labeled WT.*i* (where *i* = 1–6). Old (20 mo) WT mice are labeled Old WT.*i*. $Wrn^{\Delta hel/\Delta hel}$ mice are labeled Wrn.*i*. $Gulo^{-/-}$ mice treated with 0.01% ascorbate are labeled Gulo 0.01% ascorbate.*i*. $Wrn^{\Delta hel/\Delta hel}/Gulo^{-/-}$ mice treated with 0.01% ascorbate are labeled Wrn/Gulo 0.01% ascorbate.*i*. $Wrn^{\Delta hel/\Delta hel}/Gulo^{-/-}$ mice treated with 0.4% ascorbate are labeled Wrn/Gulo 0.4% ascorbate.*i*. The Euclidian distance and complete agglomerative methods were used for clustering.

Figure 5

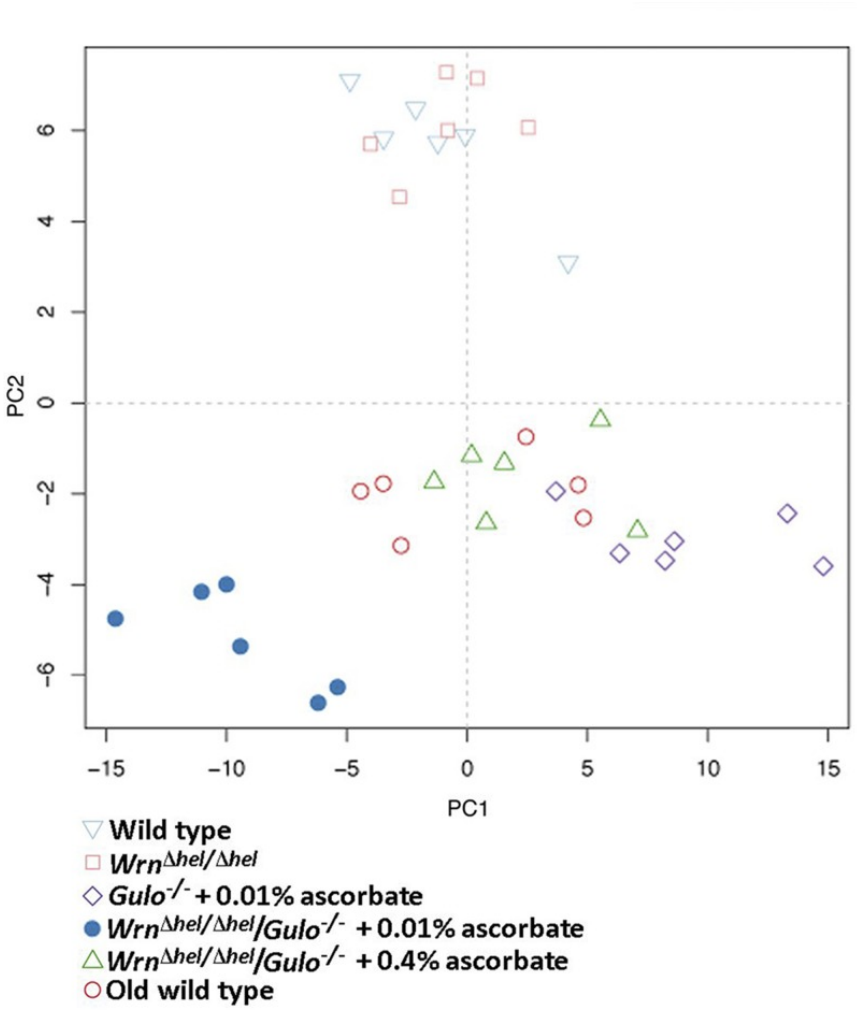

PCA graph demonstrating the differentiation effect of ascorbate and genotype on the metabolomic profiles of mice. *X* axis: principal component 1; *Y* axis: principal component 2.

Figure 6

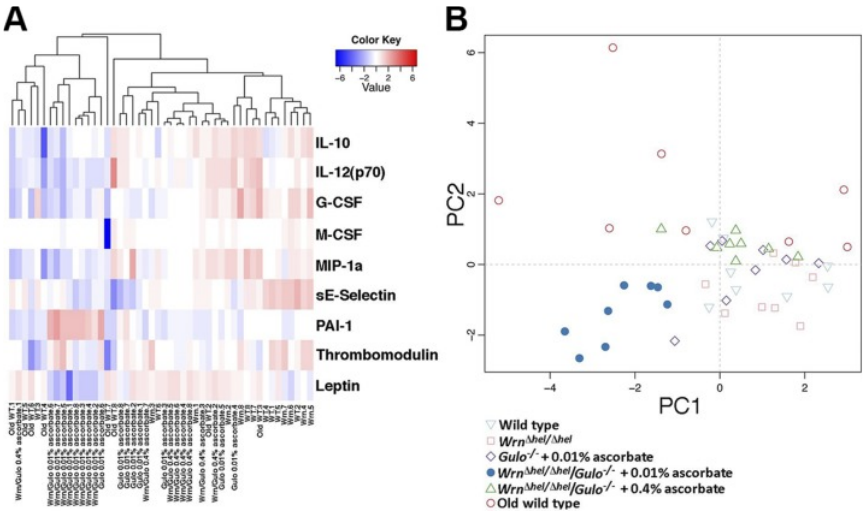

Impact of ascorbate and genotype on the cytokinome of mice. *A*) Heat map depicting the *z* score of log base 10 in serum cytokine concentrations (rows) between individual (columns) WT and mutant mice treated with different amounts of ascorbate. Significantly altered cytokines with a value of P < 0.01 are shown. Columns are reordered by hierarchical clustering by using the genotype and ascorbate treatments. The Euclidian distance and complete agglomerative methods were used for clustering. *B*) PCA graph demonstrating the differentiation effect of ascorbate and genotype on the cytokinome profiles of mice. The labels and symbols on the heat map and the PCA graph are identical to Figs. 4*A* and 5, respectively.

Figure 7

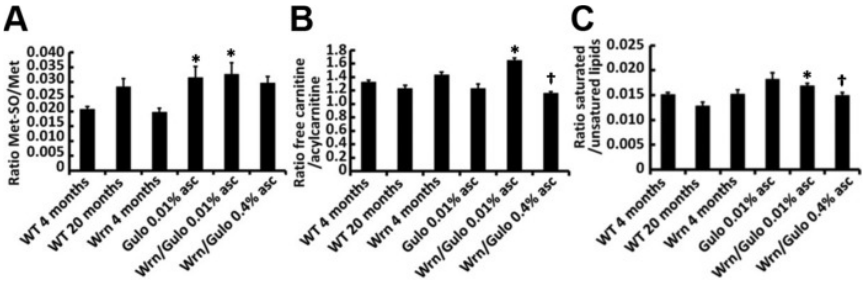

Ratios of metabolite significantly altered in $Wrn^{\Delta hel/\Delta hel}/Gulo^{-/-}$ mice. *A*) Met-SO:Met ratio. $^{*}P = 0.046$ *vs.* WT mice (by post-ANOVA Tukey test). *B*) Free carnitine (C0):acylcarnitine ratio. $^{*}P < 0.012$ *vs.* all other groups of mice and $^{\dagger}P = 0.001$ *vs.* $Wrn^{\Delta hel/\Delta hel}/Gulo^{-/-}$ mice given 0.01% supplemental ascorbate (by Tukey test). *C*) Saturated:unsaturated phosphatidylcholines ratio. Groups of mice are labeled as in Fig. 1*B*. $^{*}P = 0.021$ *vs.* WT mice and $^{\dagger}P = 0.027$ *vs.* $Wrn^{\Delta hel/\Delta hel}/Gulo^{-/-}$ mice given 0.01% supplemental ascorbate (by unpaired Student *t* tests). Bars represent SEM.

TABLE 1

Effect of the genotype and ascorbate on mitochondrial mutation rate

Genotype	Mutation/sequence (bp)[a]	Percentage	*P*[b] *Wrn*$^{\Delta hel/\Delta hel}$	*Gulo*$^{-/-}$ 0.01% ascorbate	*Wrn*$^{\Delta hel/\Delta hel}$/*Gulo*$^{-/-}$ 0.01% ascorbate	*Wrn*$^{\Delta hel/\Delta hel}$/*Gulo*$^{-/-}$ 0.4% ascorbate	Old WT (20 mo)
WT (4 mo)	19/19,693	0.096	0.3101	0.2516	0.1238	0.1061	0.0340*
Wrn$^{\Delta hel/\Delta hel}$	17/21,039	0.081	—	0.5000	0.0381*	0.2312	0.0074*
Gulo$^{-/-}$ 0.01% ascorbate	16/21,035	0.076					
Gulo$^{-/-}$			—	—	0.0259*	0.2875	0.0046*
Wrn$^{\Delta hel/\Delta hel}$/*Gulo*$^{-/-}$ 0.01% ascorbate	29/20,514	0.141	—	—	—	0.0059*	0.3042
Wrn$^{\Delta hel/\Delta hel}$/*Gulo*$^{-/-}$ 0.4% ascorbate	12/19,981	0.060	—	—	—	—	0.0011*
Old WT (20 mo)	32/19,229	0.170	—	—	—	—	—

[a]From cloned PCR fragments of mitochondrial D-loop control region. Primers are MTC1 5′-GCCAACTAGCCTCCATCTCATACTT-3′, nt 15196–15220, and MTC2 5′-GGGCGGGTTGTTGGTTTCAC-3′, nt 15701–15720.
[b]One-sided Fisher's exact test. Young WT (4 mo), old WT (20 mo), and *Wrn*$^{\Delta hel/\Delta hel}$ mice were not treated with ascorbate. *$P < 0.05$.

Figure 8

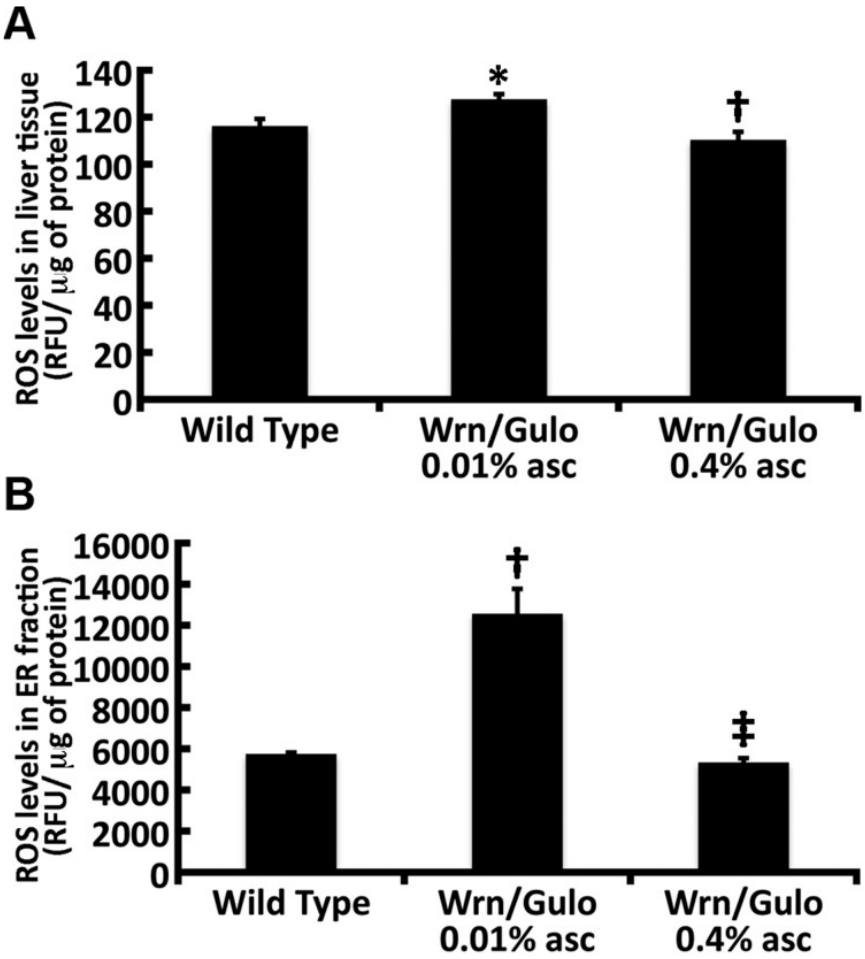

ROS levels in total liver extract and the ER enriched fraction of 4-mo-old $Wrn^{\Delta hel/\Delta hel}/Gulo^{-/-}$ mice. *A*) ROS levels in total liver extract. *$P < 0.05$ *vs.* WT mice and $^{\dagger}P = 0.01$ *vs.* $Wrn^{\Delta hel/\Delta hel}/Gulo^{-/-}$ mice given 0.01% supplemental ascorbate, by Tukey test. *B*) ROS levels in the ER enriched fraction of WT and $Wrn^{\Delta hel/\Delta hel}/Gulo^{-/-}$ mice given drinking water supplemented with 0.01 or 0.4% ascorbate. $^{\dagger}P < 0.01$ *vs.* WT mice; $^{\ddagger}P = 0.01$ *vs.* $Wrn^{\Delta hel/\Delta hel}/Gulo^{-/-}$ mice given 0.01% supplemental ascorbate (by Tukey test). ROS was detected with DCFA and is shown as relative fluorescence units (RFU). Bars in each graph represent SEM.

Figure 9

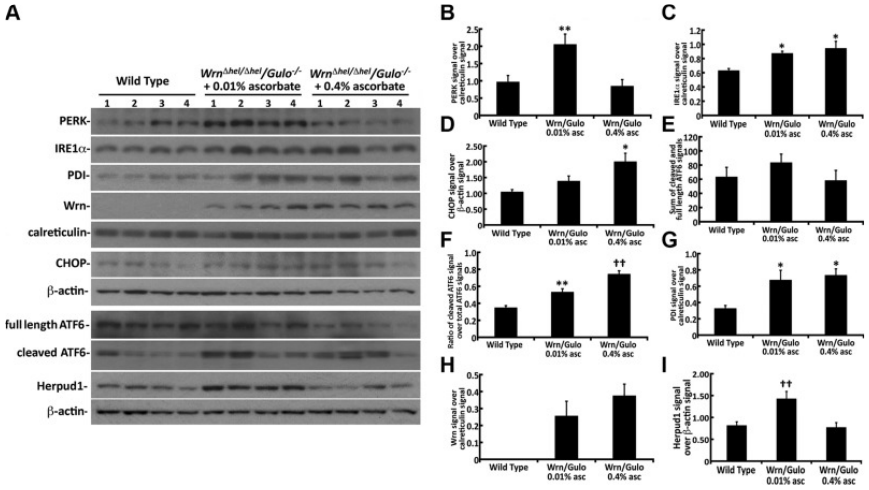

Activation of ER stress protein markers in the liver of 4-mo-old $Wrn^{\Delta hel/\Delta hel}/Gulo^{-/-}$ mice. *A*) Western blots for the indicated proteins in 4-mo-old WT and $Wrn^{\Delta hel/\Delta hel}/Gulo^{-/-}$ mice given supplemental 0.01 or 0.4% ascorbate. *B*) Ratio of total PERK signal over calreticulin signal in ER enriched fractions from the Western blots. $^{**}P < 0.05$ compared with WT and $Wrn^{\Delta hel/\Delta hel}/Gulo^{-/-}$ mice treated with 0.4% ascorbate (by Tukey post-ANOVA test). *C*) Ratio of total IRE1α signal over calreticulin signal in ER enriched fractions from the Western blots. $^{*}P < 0.05$ compared with WT mice (by Tukey post-ANOVA test). *D*) Ratio of CHOP signal over β-actin signal in total liver lysates from the Western blots $^{*}P < 0.05$ compared with WT mice (by Tukey post-ANOVA test). *E*) Sum of the cleaved and full-length ATF6 signals in total liver extracts. *F*) Ratio of the cleaved over total (cleaved and full length) ATF6 signals in total liver extracts. $^{**}P < 0.01$ compared with WT mice; $^{\dagger\dagger}P < 0.01$ compared with WT and $Wrn^{\Delta hel/\Delta hel}/Gulo^{-/-}$ mice treated with 0.01% ascorbate (by Tukey post-ANOVA test). *G*) Signal of PDI signal over calreticulin signal in ER enriched fractions from the Western blots. $^{*}P < 0.05$ compared with WT mice (by Tukey post-ANOVA test). *H*) Ratio of mutant $Wrn^{\Delta hel}$ signal over calreticulin signal in ER enriched fractions from the Western blots. *I*) Ratio of HERPUD1 signal over β-actin signal in total liver lysates from the Western blots. $^{\dagger\dagger}P < 0.01$ compared with WT and $Wrn^{\Delta hel/\Delta hel}/Gulo^{-/-}$ mice treated with 0.4% ascorbate (by Tukey post-ANOVA test). Bars in all histograms represent SEM of 4 mice.

Figure 10

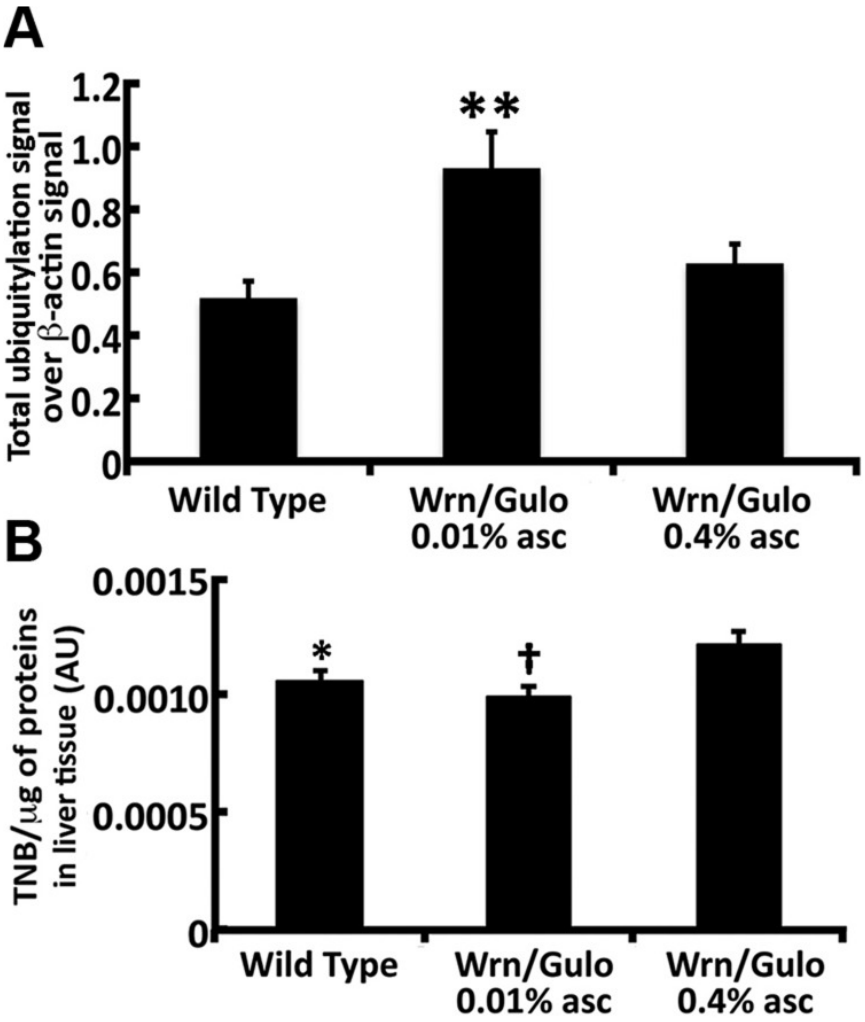

Sulfhydrylation and ubiquitylation modifications of proteins in the liver of 4-mo-old $Wrn^{\Delta hel/\Delta hel}/Gulo^{-/-}$ mice. *A*) Ratio of total ubiquitylated proteins signal over β-actin signal from the Western blots. $^{**}P < 0.05$ compared with WT and $Wrn^{\Delta hel/\Delta hel}/Gulo^{-/-}$ mice treated with 0.4% ascorbate (by Tukey post-ANOVA test). Bars in all histograms represent SEM of 4 mice. *B*) Quantification of thiol groups on proteins extracted from the liver of WT and $Wrn^{\Delta hel/\Delta hel}/Gulo^{-/-}$ mice treated with 0.01 and 0.4% ascorbate by the DTNB assay. $^{*}P < 0.05$; $^{\dagger}P < 0.01$ compared with $Wrn^{\Delta hel/\Delta hel}/Gulo^{-/-}$ mice treated with 0.4% ascorbate (by Tukey post-ANOVA test).